

12

LEVEL II

AD A066259

Technical



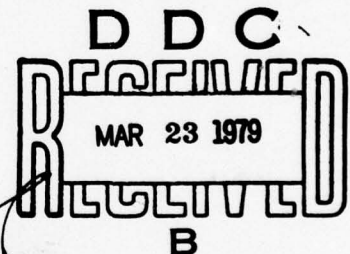
Note

TN no. N-1543

title: CEL BLAST WAVE PROPAGATION CODE FOR AIR DUCTS

author: R. S. Chapler and R. H. Fashbaugh

date: January 1979



sponsor: Omaha District Corps of Engineers, U.S. Army

program nos: 63-033



CIVIL ENGINEERING LABORATORY

NAVAL CONSTRUCTION BATTALION CENTER
Port Hueneme, California 93043

Approved for public release; distribution unlimited.

79 03 22 045

DDC FILE COPY

Unclassified

SECURITY CLASSIFICATION OF THIS PAGE (When Data Entered)

| REPORT DOCUMENTATION PAGE | | READ INSTRUCTIONS BEFORE COMPLETING FORM |
|--|-----------------------------------|---|
| 1. REPORT NUMBER TN-1543 | 2. GOVT ACCESSION NO. DN887036 | 3. RECIPIENT'S CATALOG NUMBER (9) <i>rept.</i> |
| 4. TITLE (and Subtitle) CEL BLAST WAVE PROPAGATION CODE FOR AIR DUCTS, | | 5. TYPE OF REPORT & PERIOD COVERED Final Jul 1977 - Jul 1978, |
| 7. AUTHOR(s) (10) R. S. Chapler and R. H. Fashbaugh | | 6. PERFORMING ORG. REPORT NUMBER |
| 9. PERFORMING ORGANIZATION NAME AND ADDRESS CIVIL ENGINEERING LABORATORY Naval Construction Battalion Center Port Hueneme, California 93043 | | 8. CONTRACT OR GRANT NUMBER(s) |
| 11. CONTROLLING OFFICE NAME AND ADDRESS District Engineer U.S. Army Engineer District, Omaha 6014 U.S. Post Office and Courthouse Omaha, Nebraska 68102 | | 10. PROGRAM ELEMENT, PROJECT, TASK AREA & WORK UNIT NUMBERS 63-033 |
| 14. MONITORING AGENCY NAME & ADDRESS (if different from Controlling Office) (14) CEL - TN-1543 | | 12. REPORT DATE January 1979 |
| | | 13. NUMBER OF PAGES 56 |
| | | 15. SECURITY CLASS. (of this report) Unclassified |
| | | 15a. DECLASSIFICATION/DOWNGRADING SCHEDULE |
| 16. DISTRIBUTION STATEMENT (of this Report) Approved for public release; distribution unlimited. (1264p.) | | |
| 17. DISTRIBUTION STATEMENT (of the abstract entered in Block 20, if different from Report) | | |
| 18. SUPPLEMENTARY NOTES | | |
| 19. KEY WORDS (Continue on reverse side if necessary and identify by block number) Blast, shock waves, nuclear weapons effects, air ducts, blast propagation, attenuation, computer code. | | |
| 20. ABSTRACT (Continue on reverse side if necessary and identify by block number) Refinement of a CEL hydrodynamic code for prediction of air blast propagation in variable area ventilation ducts was completed. Code solutions are one-dimensional and achieved using a refined finite-difference pseudo-viscosity method in a Lagrange formulation for solution of either classical nuclear blast waves or general time variant pressure waves. Solutions for a single constant area duct with the effects of viscosity at the wall are included. An example case is presented with a description of the single duct geometry, (continued) 7am | | |

DD FORM 1 JAN 73 1473 EDITION OF 1 NOV 65 IS OBSOLETE

Unclassified

SECURITY CLASSIFICATION OF THIS PAGE (When Data Entered)

391 111

LB

79 03 22 045

Unclassified

SECURITY CLASSIFICATION OF THIS PAGE(When Data Entered)

20. Continued

the applied nuclear blast parameters, and the code input parameters, including their magnitudes and their sources. A 2-m-diam duct with a length of 200 meters subjected to a side-on 1,000 psi overpressure is analyzed, and the time histories of the blast parameters are presented for three locations in the duct. The effects of wall friction are demonstrated graphically for friction factors of 0.016 and 0.030. Sequential application of the code to each duct in a branched duct system provides solutions for complex air entrainment systems. A description of the modified CEL Blast Wave Propagation Code basic functions, input quantities, formats and outputs (including a sample input data card listing), input data listing, and an output listing sample are appended.

Library Card

Civil Engineering Laboratory
CEL BLAST WAVE PROPAGATION CODE FOR AIR
DUCTS (Final), by R. S. Chapler and R. H. Fashbaugh
TN-1543 56 pp illus January 1979 Unclassified

1. Air ducts—Nuclear blast waves 2. Computer code—Modified hydrodynamic I. 63-033

Refinement of a CEL hydrodynamic code for prediction of air blast propagation in variable area ventilation ducts was completed. Code solutions are one-dimensional and achieved using a refined finite-difference pseudo-viscosity method in a Lagrange formulation for solution of either classical nuclear blast waves or general time variant pressure waves. Solutions for a single constant area duct with the effects of viscosity at the wall are included. An example case is presented with a description of the single duct geometry, the applied nuclear blast parameters, and the code input parameters, including their magnitudes and their sources. A 2-m-diam duct with a length of 200 meters subjected to a side-on 1,000 psi overpressure is analyzed, and the time histories of the blast parameters are presented for three locations in the duct. The effects of wall friction are demonstrated graphically for friction factors of 0.016 and 0.030. Sequential application of the code to each duct in a branched duct system provides solutions for complex air entrainment systems. A description of the modified CEL Blast Wave Propagation Code basic functions, input quantities, formats and outputs (including a sample input data card listing), input data listing, and an output listing sample are appended.

Unclassified

SECURITY CLASSIFICATION OF THIS PAGE(When Data Entered)

CONTENTS

| | Page |
|--|------|
| INTRODUCTION | 1 |
| COMPUTER CODE DESCRIPTION | 1 |
| Basic Equations | 2 |
| Finite Difference Equations | 3 |
| Boundary Conditions | 3 |
| Rezoning Method | 9 |
| Equation of State Options | 9 |
| APPLICATION OF THE CODE | 11 |
| Example Case Description | 11 |
| Input Data | 11 |
| Numerical and Graphical Results | 12 |
| Code Utilization for Systems With Branch Ducts | 14 |
| Scaling of Nuclear Burst Input Parameters | 15 |
| CONCLUSIONS | 17 |
| ACKNOWLEDGMENT | 18 |
| REFERENCES | 18 |
| APPENDIX - Lagrange Computer Code Description | 39 |
| LIST OF SYMBOLS | 50 |

| | |
|---------------------------------|---|
| ACCESSION for | |
| NTIS | White Section <input checked="" type="checkbox"/> |
| DDC | Buff Section <input type="checkbox"/> |
| UNANNOUNCED | <input type="checkbox"/> |
| JUSTIFICATION _____ | |
| BY _____ | |
| DISTRIBUTION/AVAILABILITY CODES | |
| Dist. AVAIL. and/or SPECIAL | |
| A | |

INTRODUCTION

Prediction of nuclear air blast wave propagation in air entrainment systems of hardened facilities has been the subject of extensive effort. Refinement of a Lagrange computer code prepared by the Civil Engineering Laboratory (CEL) (Ref. 1) has been completed under the sponsorship of the Omaha District Corps of Engineers, U.S. Army. This refined finite-difference hydrodynamic code using a pseudo-viscosity method in a Lagrange formulation can provide solutions for classical nuclear blast wave or other general time-variant pressure waves in air. The solutions presented in this report are for one-dimensional shock wave propagation in a constant area duct with the effects of viscosity at the duct wall included.

The CEL hydrodynamic code is capable of handling a variable area cross-section and flows with wave propagation in either direction in a duct, including shock reflection at a boundary.

Following is a description of the CEL code, including background for the finite-difference equation theory and formats for input and output. The code includes equations of state that are appropriate for air temperatures to $24,000^{\circ}\text{K}$.

Air entrainment systems having branches from the main duct may be analyzed by proper sequential application of the code to each branch.

COMPUTER CODE DESCRIPTION

The CEL hydrodynamic code is a one-dimensional variable area code which includes viscous effects at the duct wall. The code is suitable

for computation of time-dependent flows, including moving shock waves, in a single duct of either constant or variable cross sectional area. Two types of duct entrance boundary conditions can be specified at the duct inlet; the flow parameters for a classical nuclear blast wave (pressure, temperature, and dynamic pressure) or any general time variant flow state.

Duct entrance geometric configurations that can be specified are a surface side-on entry, a duct-to-duct T-junction, and a duct-to-duct Y-junction, typified in Figure 1.

The boundary condition at the exit of a duct is that of a rigid wall where particle velocity is specified as zero.

Basic Equations

The inclusion of variable area does not alter the form of either the momentum equation or the energy equation. These equations are, therefore, the same as for a constant area duct, as given in Reference 2. The momentum equation is

$$\frac{\partial u}{\partial t} = -v \frac{\partial p}{\partial x} - \frac{f}{2D} u |u| \quad (1)$$

and the energy equation is

$$\frac{\partial e}{\partial t} = -p \frac{v}{t} + \frac{f}{2D} u^2 |u| \quad (2)$$

where p = pressure

e = internal energy per unit mass

f = a wall friction coefficient

D = duct diameter

The system of equations is completed by the equation of state that, for the analysis presented here, takes the form

$$e = \frac{p V}{\gamma - 1} \quad (3)$$

Where, in the above, γ is the adiabatic exponent for a real gas. Determination of the value of γ is explained in the section on equations of state. For purposes of computation, Equations 1, 2 and 3 with the definitions for the velocity, u , and the Lagrange zone mass are written in finite difference form utilizing the pseudo-viscosity method of shock wave treatment of Reference 3.

Finite Difference Equations

The finite difference equations used to numerically integrate the set of basic equations given earlier is presented in detail in Reference 1. Also included in Reference 1 is the stability criterion that must be satisfied for the finite difference equations to be stable.

Boundary Conditions

Duct Inlet Boundary Conditions. The general computer code is capable of the following inlet boundary conditions:

- (1) A shock wave of constant strength
- (2) A shock wave of simple exponential decay

(3) A classical nuclear blast wave

(4) Any time variant flow state where pressure, temperature, and dynamic pressure are specified as a function of time

For predicting the flow environment in air entrainment systems subjected to nuclear blast waves, only boundary conditions (3) and (4) are used; therefore, these two conditions will be presented here.

To simulate nuclear blast waves where a significant negative pressure phase occurs, a simple exponential decay relationship (Equation 10 of Reference 1) is replaced by more appropriate relationships, such as those given in Reference 4. These relationships that are used in side-on entrance calculations for a surface wave are given below:

$$p_s = p_a + p_{so} \left(A_1 e^{-b_1 \tau} + A_2 e^{-b_2 \tau} + A_3 e^{-b_3 \tau} \right) (1 - \tau) \quad (4)$$

where $\tau = (t - t_s)/Dp^+$

t = time from weapon detonation as in Reference 4

t_s = shock arrival time

Dp^+ = duration of positive pressure phase

p_{so} = shock peak overpressure at $t = t_s$

The quantities A_1 , A_2 , A_3 , b_1 , b_2 , and b_3 are constants for which values are given in Reference 4 for a 1-megaton nuclear burst. In addition to a relationship for the surface pressure (p_s), relationships for the dynamic pressure (Q_s), and the temperature (T_s), are required.

$$Q_s = Q_{so} \left(A_4 e^{-b_4 w} + A_5 e^{-b_5 w} \right) (1 - w)^2 \quad (5)$$

$$T_s = T_{so} \left(\frac{t}{t_s} \right)^{b_6} \quad (6)$$

where $w = (t - t_s)/Du^+$

Du^+ = duration of positive velocity phase

Q_{so} = peak dynamic pressure at $t = t_s$

T_{so} = shock temperature at $t = t_s$

The quantities A_4 , A_5 , b_4 , b_5 , and b_6 are constants for which values are obtained from Reference 4. For defining the temperature-time history using Equation 9, the parameters T_{so} and b_6 have different values for the time intervals between t_s and the time when peak temperature is reached; for the times after the peak temperature is reached, Equations 4, 5, and 6 completely define the dynamic and thermodynamic state of the air above an inlet from which other variables can be obtained.

The total enthalpy is required for side-on entrance simulation and is defined as

$$h_{ts} = e_s + \frac{p_s}{\rho_s} + \frac{1}{2} u_s^2 \quad (7)$$

The density, ρ_s , is computed using Equations 4 and 6, and the equation of state,

$$\rho_s = \frac{p_s}{Z_s R T_s} \quad (8)$$

The parameter Z_s is a function of temperature and density and is determined as explained in the section on equations of state.

The internal energy (e_s) is determined from

$$e_s = \frac{p_s}{\rho_s (\gamma_s - 1)} \quad (9)$$

where γ_s is also a function of temperature and density.

The particle velocity (u_s) is computed using Equation 5 and the definition

$$u_s = \sqrt{\frac{2 Q_s}{\rho_s}} \quad (10)$$

Simulation of a side-on type entrance, such as that shown in Figure 1, is achieved by evaluating the flow losses from point s to point e through the use of experimental data reported in Reference 5. This flow loss is measured by the entropy increase from point s to point e. Assuming that Z , R , and γ do not change significantly from point s to point e, this entropy can be expressed in terms of state variables as

$$s_e - s_s = Z R \ln \left[\left(\frac{T_e}{T_s} \right)^{\gamma/\gamma-1} \left(\frac{p_s}{p_e} \right) \right] \quad (11a)$$

and in terms of stagnation variables as

$$s_e - s_s = Z R \ln \left[\left(\frac{T_{te}}{T_{ts}} \right)^{\gamma/\gamma-1} \left(\frac{p_{ts}}{p_{te}} \right) \right] \quad (11b)$$

In the above equations T_s , p_s , T_e , and p_e are static temperatures and pressures at points s and e, respectively, and T_{ts} , p_{ts} , T_{te} , and p_{te} are stagnation temperatures and pressures. Equating relationships (Equations 11a and 11b) yield a desired relation for the duct entrance static pressure, p_e , in the form

$$p_e = p_s \left(\frac{p_{te}}{p_{ts}} \right) \left[\left(\frac{T_e}{T_{te}} \right) \left(\frac{T_{ts}}{T_s} \right) \right]^{\gamma/\gamma-1} \quad (12)$$

In this relationship, γ is evaluated at point s. The stagnation pressure ratio (p_{te}/p_{ts}) can be expressed by the relation

$$\frac{p_{te}}{p_{ts}} = \exp (-2.3026 A_1 M_s) \quad (13)$$

where M_s is the flow Mach number at point s and A_1 is an empirical constant determined from the experimental data of Reference 5. A plot of this experimental data for the side-on entrance is shown in Figure 2 which shows the linear relationship between $\log (p_{te}/p_{ts})$ and M_s in the supersonic region of interest here. The ratio T_{ts}/T_s in relation (Equation 12) is determined directly from M_s , which is known from the given flow state at s. In order to determine the ratio T_e/T_{te} the flow Mach number at point e (M_e) must be determined. The value of M_e is evaluated

as a function of M_s , also from the data of Reference 5; therefore, T_e/T_{te} is also determined from the known value of M_s . The relationship between M_e and M_s is shown in Figure 3.

When using the computer code to predict wave propagation in a branch duct of a system, such as the horizontal duct in Figure 1, the time histories of pressure, temperature, and dynamic pressure are required at the inlet boundary to this branch duct. These time histories are provided in the code in the form of polynomials. Specifically, the pressure, the temperature, and the dynamic pressure are in the form

$$\begin{aligned} p_s &= a_0 + a_1 t + a_2 t^2 + \dots + a_7 t^7 \\ Q_s &= b_0 + b_1 t + b_2 t^2 + \dots + b_7 t^7 \\ T_s &= c_0 + c_1 t + c_2 t^2 + \dots + c_7 t^7 \end{aligned} \quad (14)$$

For this case, Equation 14 replaces Equations 4, 5, and 6, and the remaining Equations 7 through 13 are the same as for the nuclear case.

The value of the empirical constant A_1 in Equation 13 depends upon the geometrical configuration at the duct entrance; e.g., a side-on entrance, a T-junction, or a Y-junction. To determine accurately the values of A_1 , the transmitted shock strength calculated by the code was obtained for four values of A_1 with an incident shock overpressure of 1,000 psi. The results are shown in Figure 4 with the values of A_1 that will yield a transmitted shock overpressure in agreement with the data of Reference 5.

Duct Exit Boundary Conditions. The boundary condition at the exit end of a duct is considered a closed-end condition because the particle velocity at that point will remain zero. The finite difference form of this boundary condition is given in Reference 1.

Rezoning Method

The finite difference equation options for the entrance interface are such that flow directions can reverse, and outflow can occur when the surface pressure becomes less than the pressure in the duct.

When a new zone is formed at the duct entrance, the internal energy of the new zone is determined by assuming the total enthalpy at points s and e are equal. This assumption yields

$$e_e = \frac{1}{\gamma_e} (h_{ts} - \frac{1}{2} u_e^2) \quad (15)$$

where h_{ts} is the total enthalpy at point s. The equation of state has been used in obtaining Equation 15. The value of h_{ts} is known, since values for all shock parameters are known at point s; it is given by Equation 7. The value of u_e is, however, unknown and is approximated by the value calculated during the previous time cycle. An iteration technique could be used to improve the value used for u_e , but a comparison of computed results with experimental data showed this to be unnecessary (Ref 2). The pressure in the new zone is initially assumed as the mean between the inlet pressure (p_e) and the pressure in the second zone. This approximate method for establishing a new inlet zone to allow mass inflow yields a result for the shock peak pressure that is approximately 5% high and a shock speed that is approximately 2% high. A more detailed discussion of rezoning is given in Reference 1. Adjustment of the entrance loss coefficient (A_1) as previously explained, reduces these errors and more closely matches the predicted peak pressure with the experimental data.

Equation of State Options

Two equation of state subroutines are available in the CEL computer code: (1) the equation of state for an ideal gas that is accurate for

temperatures up to 1,000°K and (2) a real gas equation of state that is accurate for temperatures up to 24,000°K. The basic theory upon which these subroutines are based is given below.

Perfect Gas Equation of State. The equation of state for an ideal gas can be written in the form:

$$p = \rho R T \quad (16)$$

where p = pressure

ρ = density

R = particular gas constant

T = absolute temperature

Because of the computational advantages offered by the use of Equation 16, most problems of shock transmission through gases are solved using the ideal gas law. Moreover, the ideal gas law yields simple analytical relationships between the various shock parameters. The thermally and calorifically perfect gas is, however, an idealization; and real gases, depending on their temperature and pressure, will deviate from it to varying degrees. It has been noted from experience (Ref 6) that the ideal gas law predicts the shock flow parameters with good accuracy up to temperatures of 1,000°K. However, at higher temperatures, the number of particles per unit mass and, hence, the average molecular weight of the gas may change due to molecular dissociation, chemical reactions, and ionization. Thus, when computing flow parameters for shocks through gases at high temperatures and moderately high pressures, the ideal gas equation must be modified to include the contributions by additional degrees of freedom to the energy of the gas molecules that were not excited at low temperatures.

Real Gas Equation of State. The real gas equation of state can be written in the form:

$$p = \rho Z R T \quad (17)$$

where Z is the compressibility factor, which is a function of temperature and density and is equal to 1 for temperatures below 1,000°K and is greater than 1 for temperatures above 1,000°K. The manner in which Z varies with temperature up to 24,000°K and with density is determined from the data of Reference 6 and is also given in Reference 1.

APPLICATION OF THE CODE

Example Case Description

For the example case shown in Figure 5, a single vertical duct 2 meters in diameter and 200 meters long is subjected to a 1,000 psi overpressure generated by detonation of a 1-megaton nuclear weapon (surface burst). An ambient pressure of 14.7 psia and temperature of 59.3°F are assumed. The locations for which the blast wave histories are desired are designated by the symbols "G," "F," and "3." Their distances from the duct inlet are 0.95, 181, and 195 meters, respectively.

Input Data

Input data required for the example case was obtained from Reference 4 and the curves of Figures 2, 3, and 4 of the text. The data are presented in Table 1 with their code symbols, values, references, and remarks on methods of estimating the values, as necessary. A data card listing (Table 3 in the Appendix) is presented for the example case. Dimensions for the input data are in the cgs (centimeter-gram-second) system. Temperatures are in degrees Kelvin, and code inputs for the

surface temperature time history are obtained as indicated in Figure 6. This time history is approximated by the two linear curves I and II as shown in the figure. The axis intercepts and slopes required for the linear equations are as shown.

Selection of station locations where the distance from inlet to station is less than five zone lengths will produce inaccurate results. Location of stations at distances greater than five zone lengths is recommended. If a station location nearer than five zone lengths is necessary, then it is recommended that the number of zones be increased. The greater number of zones will increase the computer running time somewhat, but the results obtained will not be subject to the errors found otherwise. Location of the stations should be such that they will fall at the center of the length of the original zone nearest to the point of interest in the duct.

In use of the data of Table 1, the values selected for the friction factor (FRICT) were used in sequence to compute the time histories of pressure, temperature, dynamic pressure, density, and flow velocity at three stations identified as G, F, and 3 in Figure 6. The assigned friction factors were 0.016, for smooth-walled ducts, and 0.030, for somewhat rough-walled ducts. Although selection of these friction factors was not the subject of study, it has previously been shown that the 0.016 value used matched shown tube experimental data very closely.

Numerical and Graphical Results

Computer numerical results are presented in Table 5 (see the Appendix). Predicted blast wave parameters were printed every 100 cycles by setting NPR equal to 100. At each NPR cycle, the time of the numbered cycle and the length of the next timestep were printed.

Next, a single line of eight columns was printed giving in cgs dimensions, the values of the overpressure (PS), the dynamic pressure (QS), the temperature (TEMPS), the compressibility (ZS), the ratio of

specific heats (GAMMAS), the total enthalpy (HTS), the density (DS), and the internal energy (ES) of the gas at the duct side-on entrance inlet at the beginning of the cycle.

The tabulation of each zone center location and the state parameters of the gas in the zone is next presented in a 15-column format. For each zone, one line is given. In the sample shown in Table 5 - for the 500th cycle - of the 113 used only 68 zones are listed. An original assignment of 100 zones was made; therefore, an additional 13 zones had been created by the code to accommodate the inflow of gas from the blast wave into the duct. The change in gas state parameters in the zones further from the inlet than the 68th had not yet been affected by the shock wave and were the same as originally specified; therefore, printout was suppressed automatically. In succeeding cycles the blast wave progressed farther into the duct, and all the zones were found to have state parameters significantly different from those originally assigned.

At the end of each tabulation the number of zones existing is given and the locations of the maximum pseudo-viscosity (PQ) and the maximum overpressure (PSI) are given. The point of maximum pseudo-viscosity is the shock wave location. The time histories of pressure, dynamic pressure, and temperature for the three duct locations G, F, and 3 (Figure 5) are presented graphically in Figures 7 through 9. Comparison of Figures 7a and 7b shows the attenuation of the primary wave front and magnitude of the wave reflected from the end of the duct. The effect of the increase in the friction factor from 0.016 to 0.030 is readily seen. The dynamic pressure curves in Figure 8 show how rapidly the dynamic pressure decays for the primary wave. These curves do not reveal much in the way of insight of the problem but are necessary when specifying the inlet flow state to a branch duct. The temperature history of Figure 9a shows the temperature rise due to the shock front followed by a slower rise due to the nuclear radiation effects. Figure 9b indicates that the interface of hot gas entering the duct did not reach station F. In fact, as Figure 10 shows, the maximum penetration into the duct of the hot gases was 167.5 meters. The primary wave had reflected from the

duct end and reached the hot gas interface, reversing its direction of flow before the interface reached station F. Also in Figure 10 is shown the gas temperature upstream of the hot gas interface and the temperature rise across the interface.

Code Utilization for Systems With Branch Ducts

Branch ducts are those ducts which intersect the main duct and may be described as forming one element of a T- or Y-junction (Figure 1). To analyze the blast wave propagation in branch ducts requires a different set of code inputs than that required for the nuclear blast incident on the main duct shown in the example case (Figure 5). For example, at the entrance to the horizontal duct of Figure 1, the pressure waveform will show two shock fronts - the initial shock front followed by a reflected shock front, as shown in Figure 7b. The temperature and dynamic pressure (or velocity) waveforms, which are required in addition to the pressure to specify the flow state, will also be complex because of the two shock fronts, as shown in Figures 8b and 9b. The OUT3 subroutine of the CEL computer code provides these waveforms from which analytical expressions can be derived for the pressure, temperature, and dynamic pressure which serve as the input data for the horizontal duct solution.

The inputs to the horizontal duct are calculated with the vertical duct only and, thus, without the T-junction. Therefore, the input waveforms for the horizontal duct are approximations. The initial shock front, however, is exactly the same as it would be if the T-junction were in the system since the shock speed is supersonic and, therefore, not affected by the downstream configuration. The second shock front of the horizontal duct input is due to the initial shock passing the T-junction, reflecting from the end of the vertical duct and returning to the T-junction. This shock front will be stronger in the analysis than in the actual case since an approximate 10% transmission loss

through the T-junction is neglected. The result is, therefore, a conservative input to the horizontal duct with the primary shock accurate and the secondary or reflected shock higher than actual.

An analysis of the horizontal duct, analyzed as a single duct without the Y-junction (Figure 1), provides the input waveforms for the branch duct. Since the Y-junction is omitted in this calculation the initial shock at this junction will be accurate but the reflected shock from the blast valve will be higher than actual by approximately 10%.

In summarizing this procedure it is seen that, using Figure 1 as an example, successive use of the code to analyze each of the ducts results in the initial shock accurate to the T-junction of the vertical duct, accurate to the Y-junction in the horizontal duct, and accurate throughout the branch duct from the Y-junction. The reflected shock from the debris pit and from the blast valve will be approximately 10% higher than actual.

The input waveforms for the branch duct are provided by 7th-order polynomials, which are determined by standard curve-fitting techniques. In the code a zero value for TMPS2 calls the option for these polynomial waveforms in place of the nuclear surface wave inputs. The input constants for these polynomials are explained in Table 2 (see the Appendix).

Scaling of Nuclear Burst Input Parameters

Methods for scaling of nuclear blast parameters for weapon yields other than 1 megaton and 1,500 feet are given in References 4 and 7. The following scaling relationships are given for the convenience of the reader.

Code input parameters may be estimated according to scaling laws for nuclear blast parameters, as in the following:

$$p_{so} = 3000 \frac{W}{R^3} + 192 \left(\frac{W}{R^3} \right)^{1/2} \quad (18)$$

where p_{so} = overpressure in ksi

W = weapon yield in kilotons

R = range from a surface burst ground zero in kilofeet

$$Q_{so} = \frac{5}{2} \left(\frac{p^2}{7 p_o + p} \right) \quad (19)$$

where Q_{so} = dynamic pressure in psi

p = overpressure in psi

p_o = ambient pressure in psia

$$t_s = t_{s1} \left(\frac{W}{W_1} \right)^{1/3} \quad (20)$$

where t_s = shock arrival time in seconds at range R

t_{s1} = shock arrival time at range R for a 1 megaton yield

W = weapon yield

The positive phase durations D_p^+ and D_u^+ also scale according to the cube root of the weapon yield as in Equation 20 for t_s .

The constants and exponents that determine the analytic forms for overpressure and dynamic pressure for the nuclear wave depend on the value of overpressure only and can be obtained from Reference 4 for any weapon yield.

The analytic form for the temperature-time history was given previously (Equation 6). The constants T_{so} and b_6 depend upon weapon yield for a given range, and it is necessary to know the temperature-time history for the desired yield. Temperature estimation for yields other than 1 megaton is limited. However, the temperature history for a desired weapon yield can be estimated, using the 1-megaton curves of temperatures versus range given in Figures 2 and 5 of Reference 4, and scaling the shock arrival times according to Equation 20. A curve such as that given in Figure 6 of this report can then be constructed for a desired range by cross-plotting of the scaled curves. The temperature rise at the shock front is known for a given overpressure, and the estimated temperature after the shock front affects only the temperature rise across the contact surface or hot gas-cold gas interface. The strength of the shock wave in the duct is not affected by this estimation.

CONCLUSIONS

The CEL computer code can be used to calculate the propagation of blast waves in air ducts of constant or variable cross section. Branched ducts may be analyzed by sequential application to each branch. Peak overpressures of reflected waves which follow the primary wave in a branch are somewhat higher than the real case because some energy losses of the reflected wave at the branch inlet junction are neglected. However, all losses in the primary wave are included at a branch inlet. Blast wave attenuation due to friction is slightly lower than the experimental data, but selection of a more appropriate variable friction factor will improve the prediction as additional shock attenuation experimental data become available. For example, the predicted overpressure is approximately 20% lower than the measured value at a distance down a shock tube where the length-to-diameter ratio is 300 and the shock overpressure at the inlet to the shock tube is 400 psi (for a friction factor value of 0.016). The CEL computer code is efficient; therefore, blast wave propagation in a long duct can be predicted with

moderate computer running time. For example, for a 6-ft-diam duct 2,500 feet long and an inlet overpressure of 250 psia, the computer running time is about 40 seconds using a CDC6600 computer.

The CEL computer code gives the air entrainment system designer a means for estimating blast wave propagation in any duct system for blast waves generated either by nuclear or high explosive weapons or by explosion-driven blast waves from any cause where the incident waveforms can be described by up to three 7th-order polynomial equations for the pressure, the dynamic pressure, and the temperature.

ACKNOWLEDGMENT

The very difficult computer programming required in the development of the CEL Blast Wave Propagation Code was done by Mrs. Rita Brooks of CEL.

REFERENCES

1. Civil Engineering Laboratory. Technical Report R-820: Nuclear shock wave propagation through air entrainment systems of hardened facilities, by R. Fashbaugh and A. Widawsky. Port Hueneme, Calif., Apr 1975.
2. Naval Civil Engineering Laboratory. Technical Note N-1205: Shock wave propagation through air entrainment systems - Phase I, by R. H. Fashbaugh and A. Widawsky. Port Hueneme, Calif., Feb 1972.
3. R. D. Richtmyer and K. W. Morton. Difference methods for initial-value problems, 2nd ed. New York, N.Y., Interscience Publishers, 1957, pp 288-388.

4. The Rand Corporation. Report No. R-425-PR: A review of nuclear explosion phenomena pertinent to protective construction, by H. L. Brode. Santa Monica, Calif., May 1964.

5. Ballistic Research Laboratories. Memorandum Report No. 1390: Information summary of blast patterns in tunnels and chambers, by Shock Tube Facility Staff. Aberdeen Proving Ground, Md., Mar 1962.

6. The Rand Corporation. Research Memorandum RM-1543: Equilibrium composition and thermodynamic properties of air to 24,000^oK, by F. R. Gilmore. Santa Monica, Calif., 24 Aug 1955.

7. Air Force Weapons Laboratory. AFWL-TR-74-102: The Air Force manual for design and analysis of hardened structures, by R. E. Crawford, C. J. Higgins, and E. H. Bultman. Albuquerque, N.M., Civil Nuclear Systems Corporation, Oct 1974.

Table 1. Example Case Input Data

| Code Symbol | Value | Source Symbol | Source | Remarks |
|----------------|-----------|-----------------|------------------|-----------------------------------|
| A ₁ | 0.15 | a | Ref. 4, pp 33-34 | See Figure 24 of reference |
| A ₂ | 0.30 | b | Ref. 4, pp 33-34 | See Figure 24 of reference |
| A ₃ | 0.55 | c | Ref. 4, pp 33-34 | See Figure 24 of reference |
| A ₄ | 0.32 | d | Ref. 4, pp 33-34 | See Figure 24 of reference |
| A ₅ | 0.68 | f | Ref. 4, pp 33-34 | See Figure 24 of reference |
| B ₁ | 2.9 | α | Ref. 4, pp 33-34 | See Figure 24 of reference |
| B ₂ | 21.0 | β | Ref. 4, pp 33-34 | See Figure 24 of reference |
| B ₃ | 130.0 | γ | Ref. 4, pp 33-34 | See Figure 24 of reference |
| B ₄ | 150.0 | ζ | Ref. 4, pp 33-35 | See Figure 25 of reference |
| B ₅ | 350.0 | ϕ | Ref. 4, pp 33-35 | See Figure 25 of reference |
| B ₆ | 1.99 | - | Ref. 4, p. 9 | See Figure 6 for slope of line I |
| B ₇ | -0.6314 | - | Ref. 4, p. 9 | See Figure 6 for slope of line II |
| DP | 1.2 sec | Dp [†] | Ref. 4, pp 33-34 | See Figure 30 of reference |
| DU | 2.5 sec | Du [†] | Ref. 4, pp 33-35 | See Figure 30 of reference |
| TS | 0.08 sec | t _s | Ref. 4, p. 32 | See Figure 23 of reference |
| TB | 0.163 sec | - | Ref. 4, p. 9 | See Figure 6 of text |
| PSO | 1000 psi | P _s | Ref. 4, pp 33-34 | |
| QSO | 2900 psi | Q _s | Ref. 4, pp 33-34 | See Figure 23 of reference |

(continued)

Table 1. Continued

| Code Symbol | Value | Source Symbol | Source | Remarks |
|-------------|-------------------------------------|---------------|--------------|---|
| TMPS1 | 2,800°K | ΔT_s | Ref. 4, p 39 | See Figure 29 of reference |
| TMPS2 | 63,600°K | - | Ref. 4, p 9 | See Figure 6 of text |
| AI | 0.49 | - | Text | Figure 4 |
| I | 1 | - | Text | Number of ducts under consideration |
| NEQST | 3 | - | Text | Equation of state in duct |
| JCALC | 5 | - | Text | Number of last interface calculated |
| NZONES | 100 | - | Text | Number of zones assigned in duct |
| KOUT3 | 3 | - | Text | Number of locations for stored P-T data |
| GAMMAI | 1.4 | γ | Text | Initial value of specific heat ratio |
| OUTBDY | 20,000 cm | - | Text | Duct length |
| EINIT | 2.068×10^9 ergs/gram | - | Text | Initial internal energy of undisturbed air |
| UINIT | 0.0 cm/sec | - | Text | Initial velocity of undisturbed air in duct |
| DINIT | 1.2256×10^{-3} grams/cu cm | - | Text | Initial density of undisturbed air in duct |
| FRICT | 0.016 or 0.030 | - | Text | Smooth wall coefficient of friction Rough wall coefficient of friction |
| CINQ | 2.0 | - | Text | Pseudo-viscosity constant |
| AINQ | 0.2 | - | Text | Pseudo-viscosity constant |
| DO | 200 cm | - | Text | Diameter of duct |

(continued)

Table 1. Continued

| Code Symbol | Value | Source Symbol | Source | Remarks |
|-------------|-----------|---------------|--------|--|
| D1 | 0 | - | Text | Linear rate of change of duct diameter |
| D2 | 0 | - | Text | Not used |
| D3 | 0 | - | Text | Not used |
| X1 | 0 | - | Text | Distance, inlet to transition start. |
| X2 | 0 | - | Text | Distance, inlet to transition end |
| S1 | 950 cm | - | Text | Distance, inlet to specified locations |
| S2 | 18,100 cm | - | Text | where blast wave parameters (pressure- |
| S3 | 19,500 cm | - | Text | temperature data) are to be obtained |

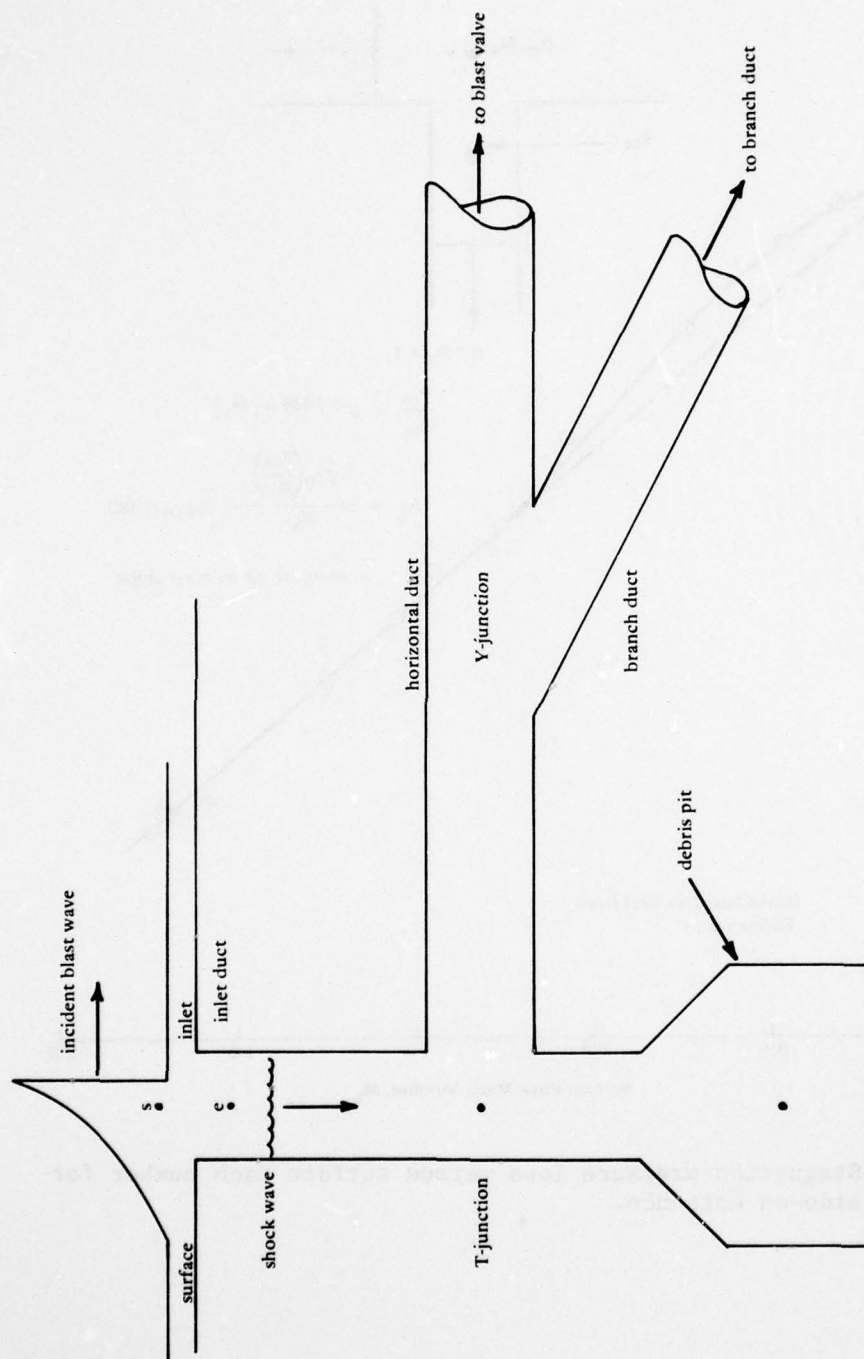


Figure 1. Typical air entrainment system.

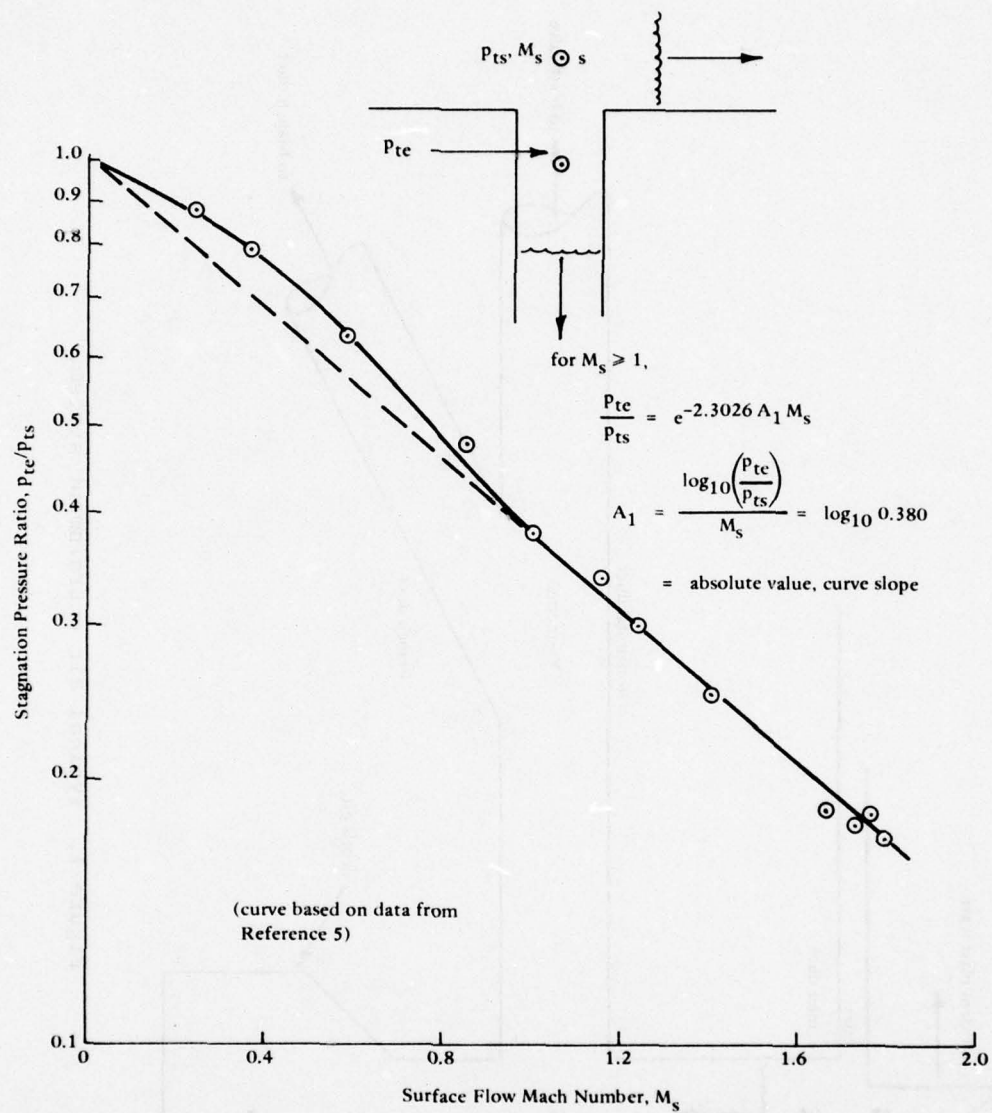


Figure 2. Stagnation pressure loss versus surface Mach number for side-on entrance.

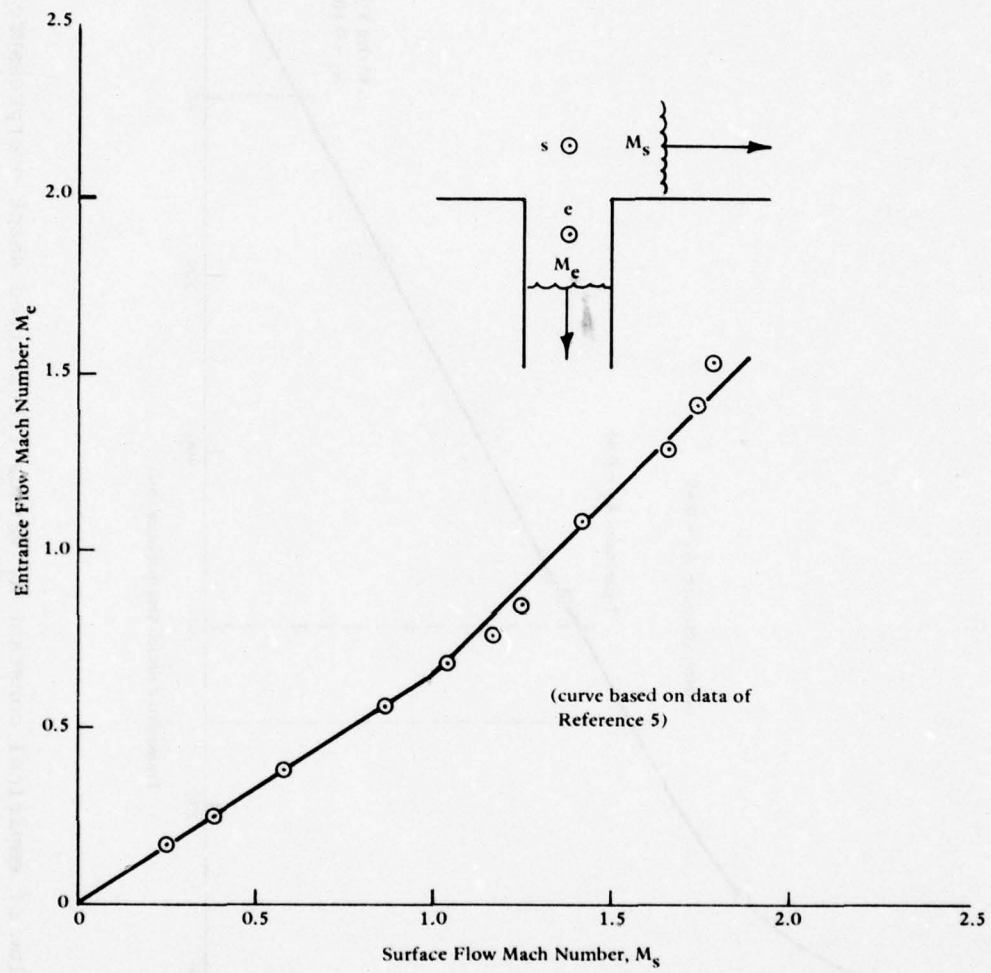


Figure 3. Surface flow Mach number versus entrance flow Mach number for side-on entrance.

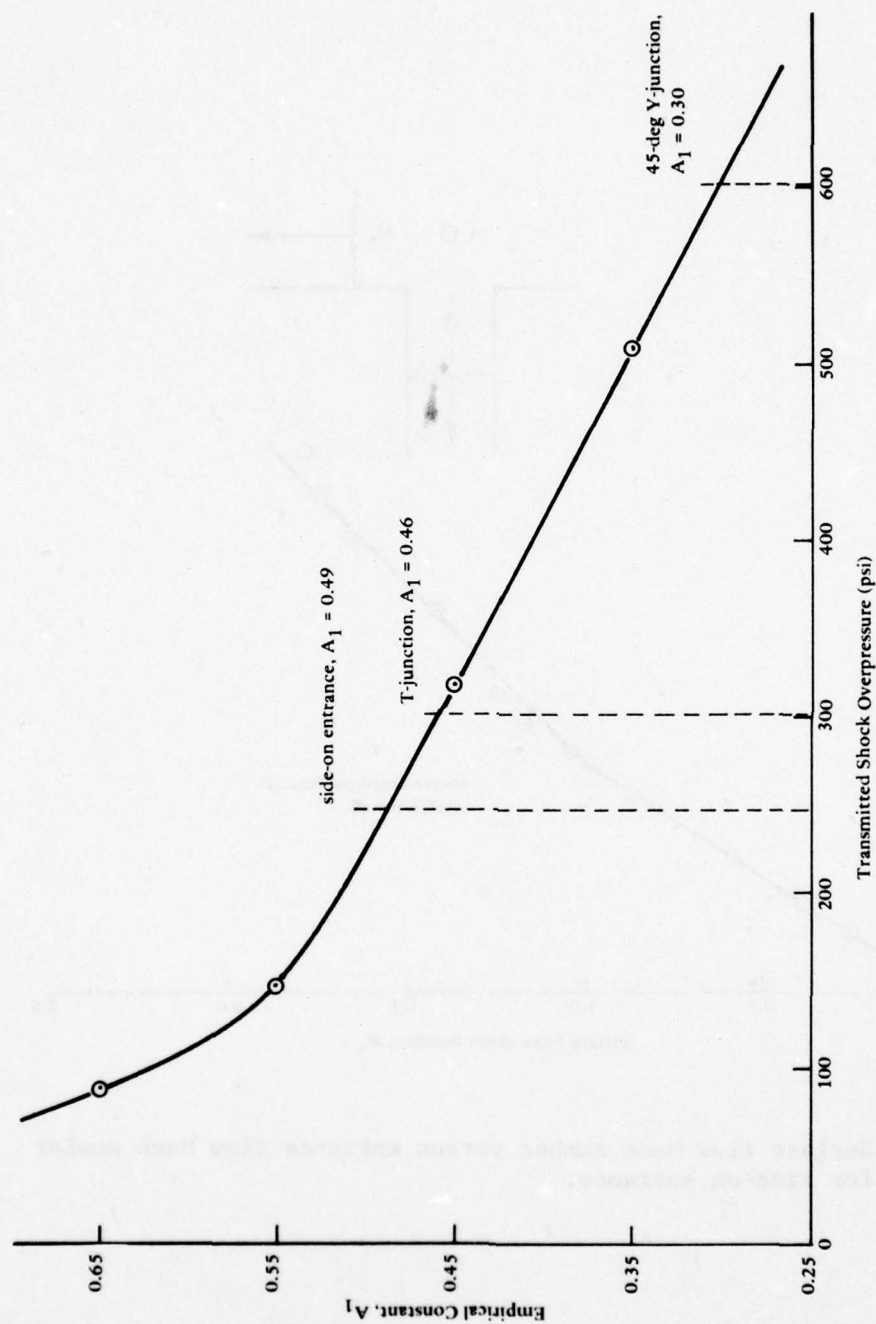


Figure 4. Value of empirical constant A_1 versus transmitted shock overpressure for incident shock overpressure of 1,000 psi.

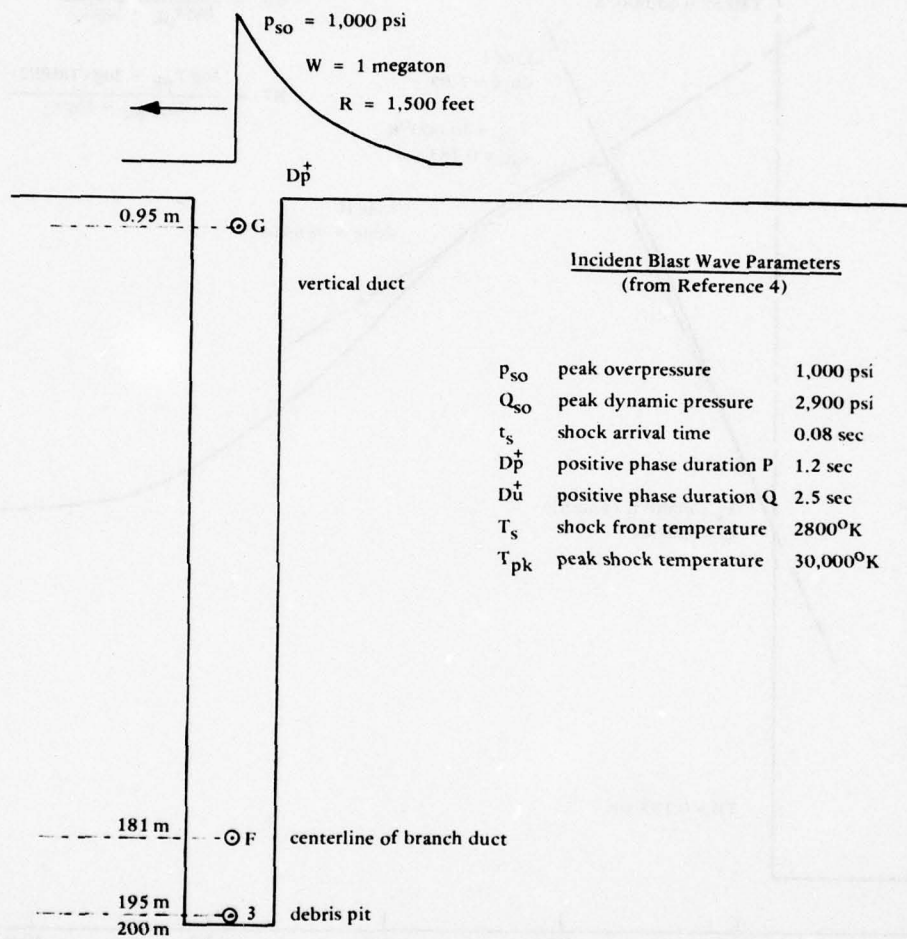


Figure 5. Example case of geometry and blast wave characteristics.

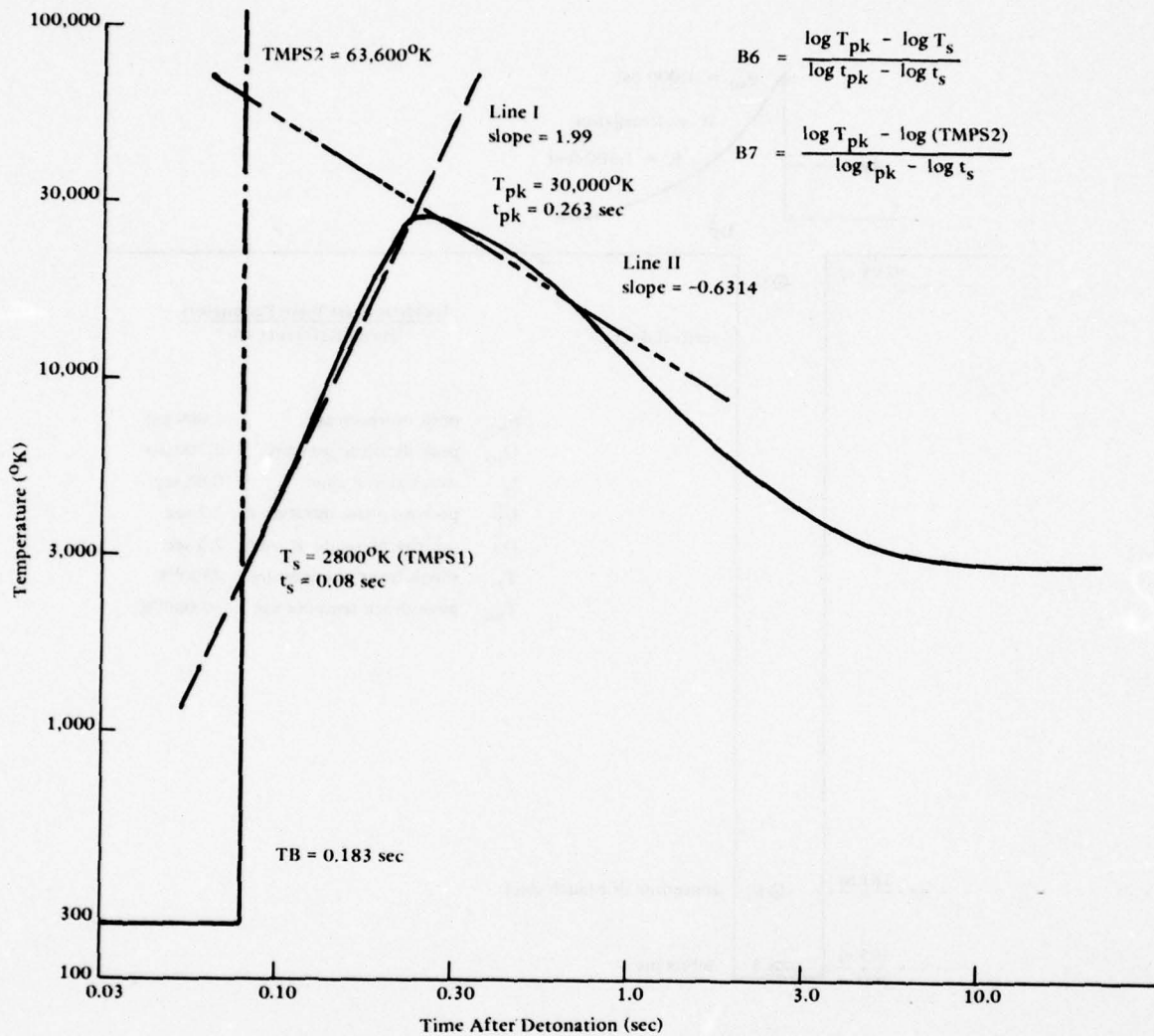


Figure 6. Estimation of temperature coefficients for input data of example case.

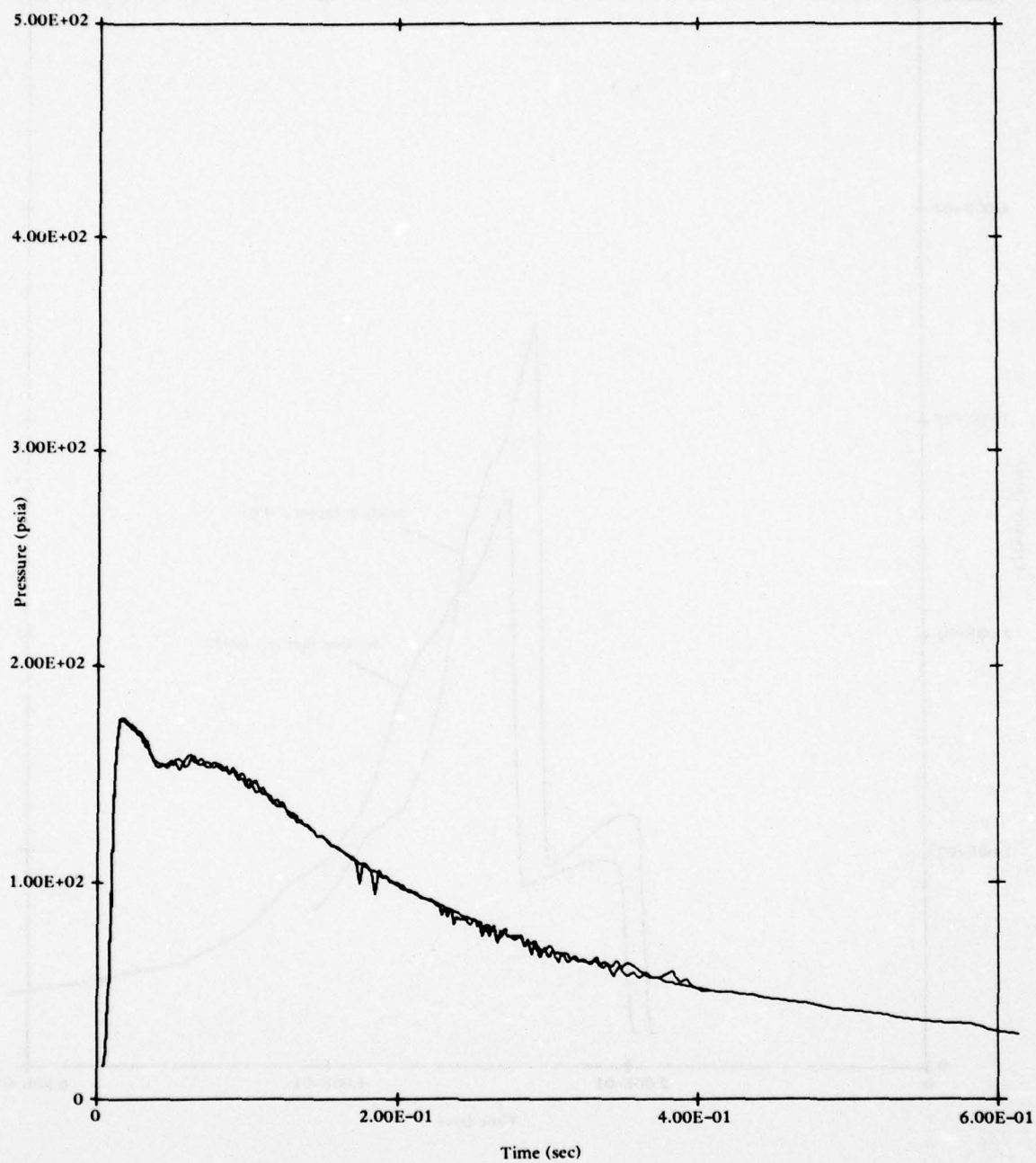


Figure 7a. Pressure-time history for duct inlet station G.

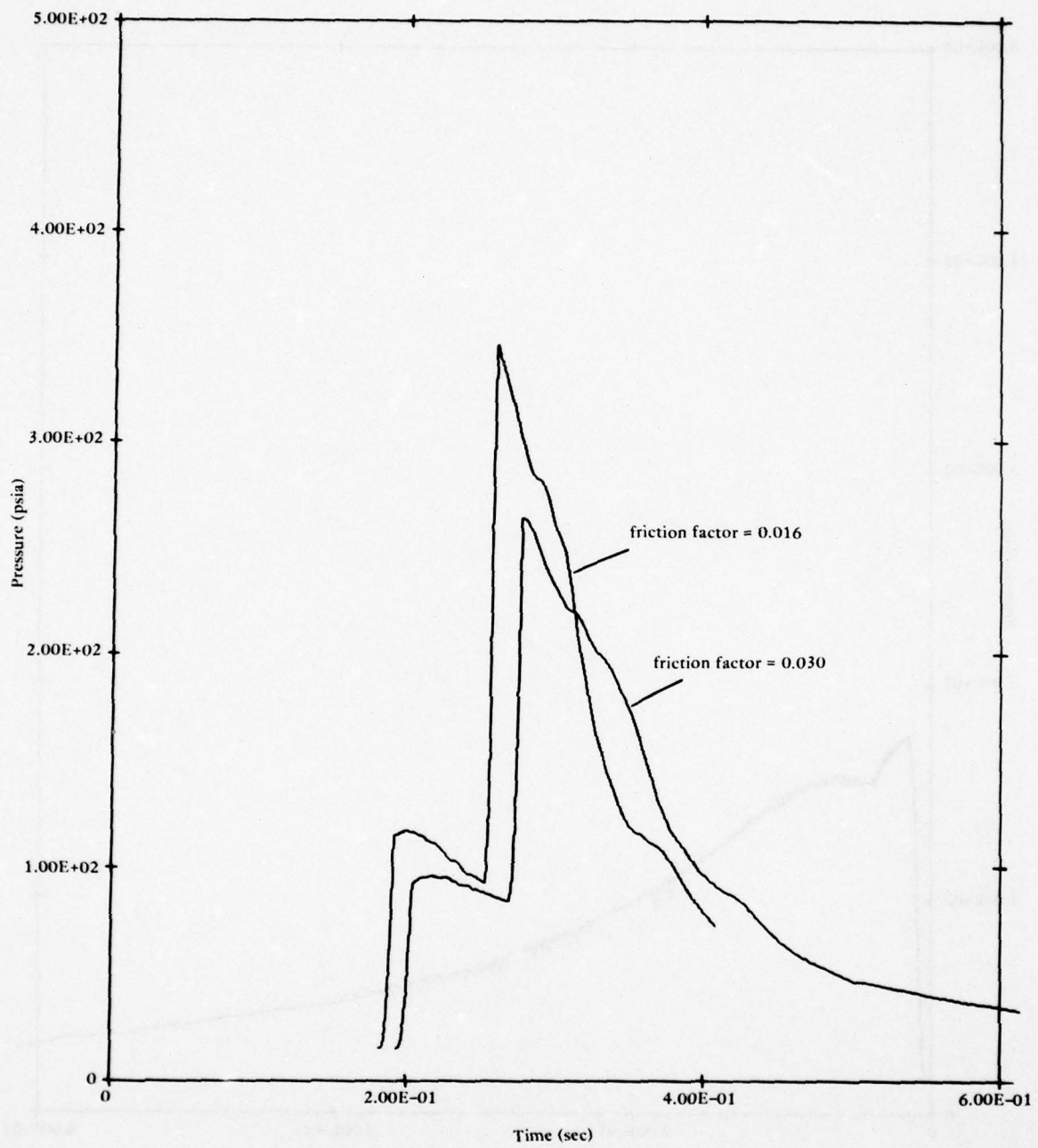


Figure 7b. Pressure-time history for duct station F.

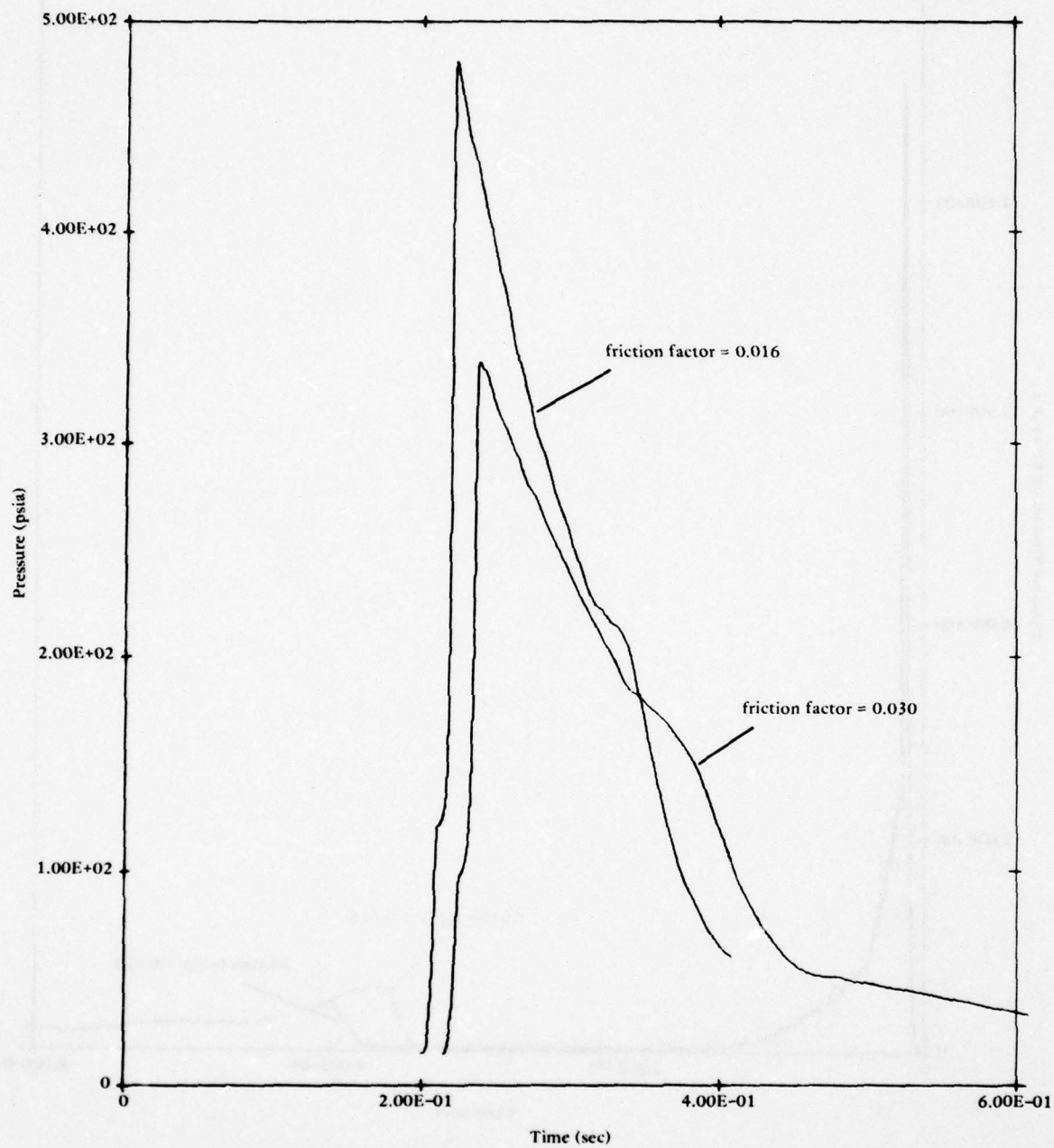


Figure 7c. Pressure-time history for duct station 3.

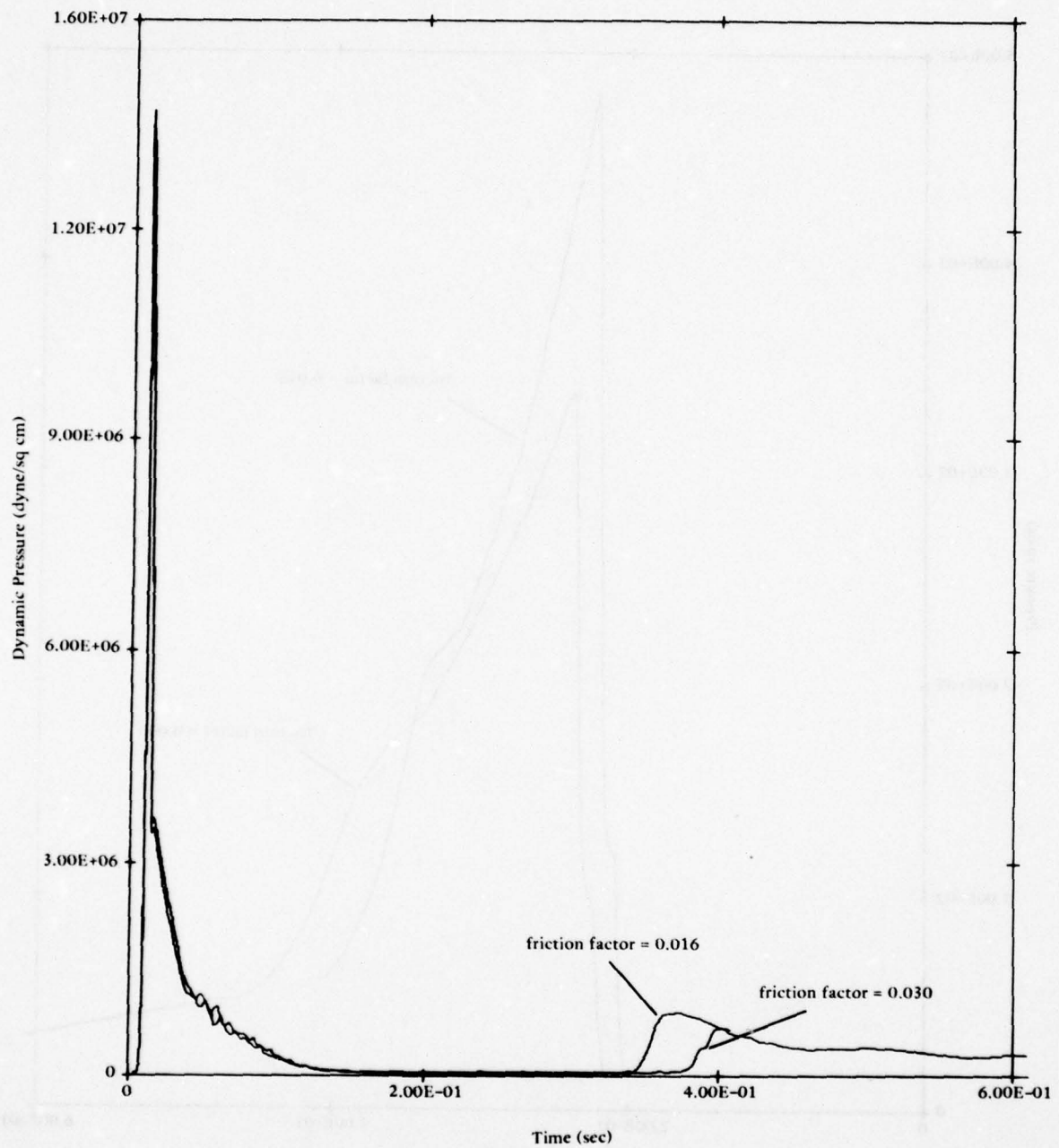


Figure 8a. Dynamic pressure-time history for duct inlet station G.

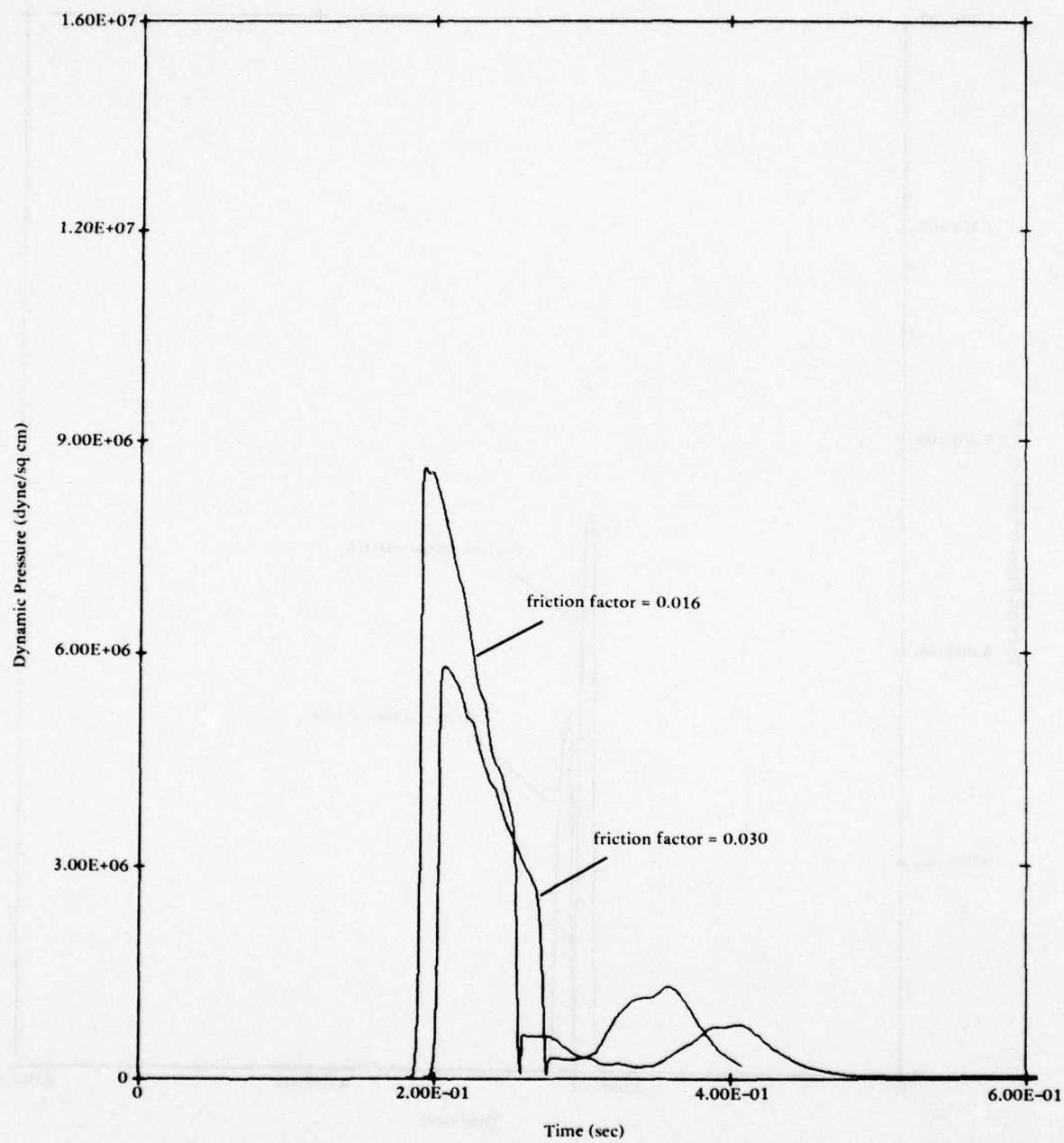


Figure 8b. Dynamic pressure-time history for duct station F.

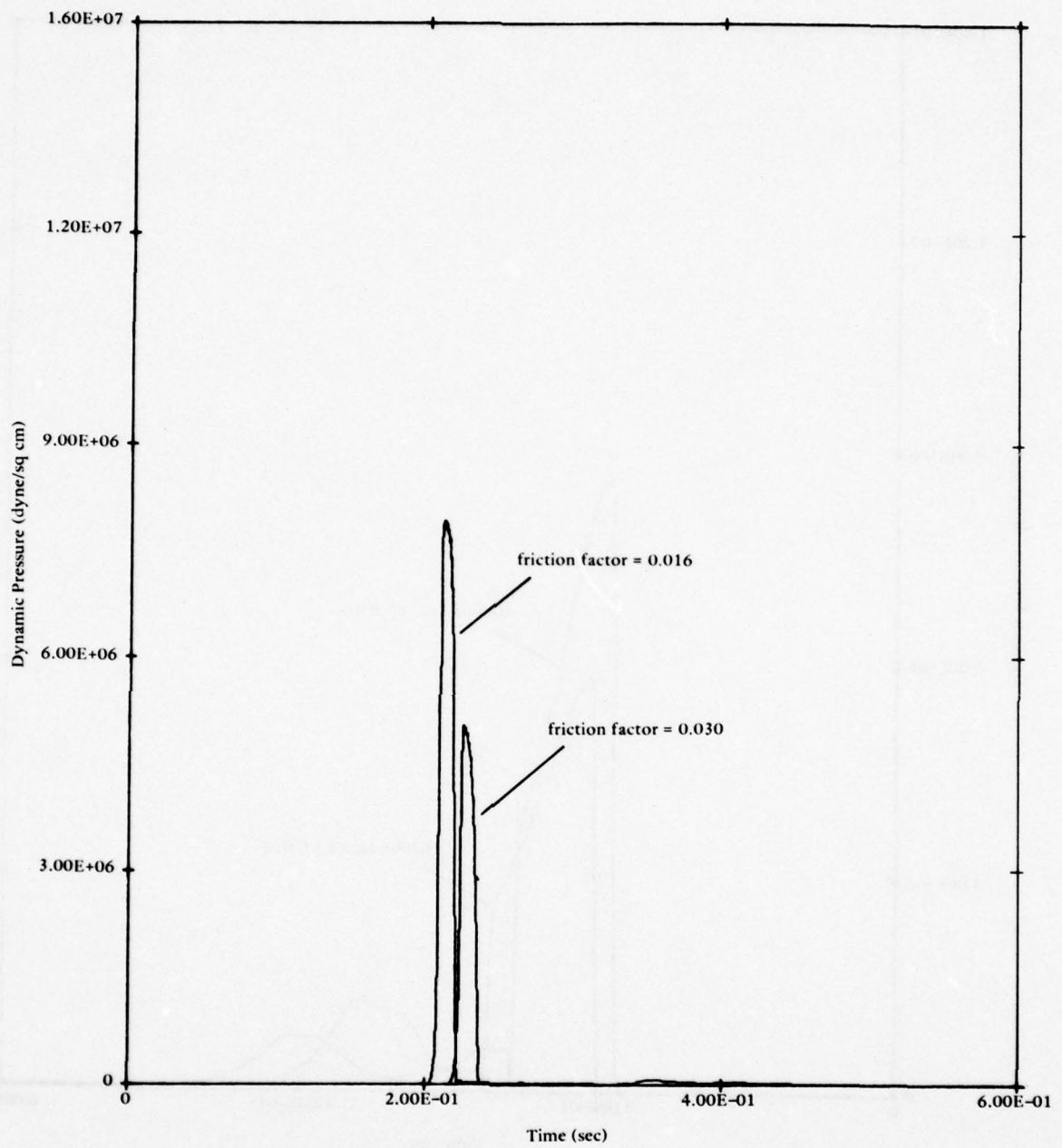


Figure 8c. Dynamic pressure-time history for duct station 3.

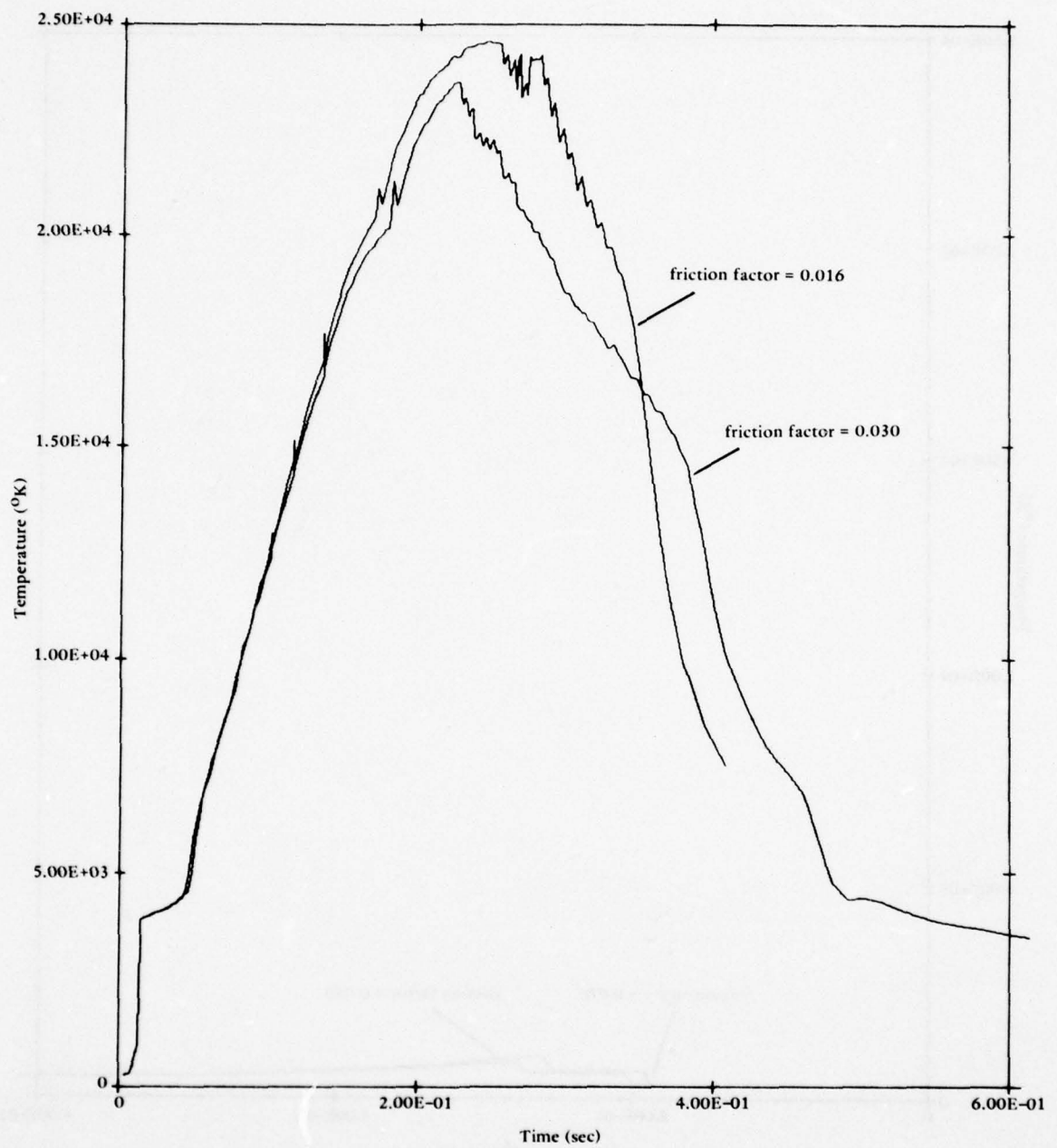


Figure 9a. Temperature-time history for duct inlet station G.

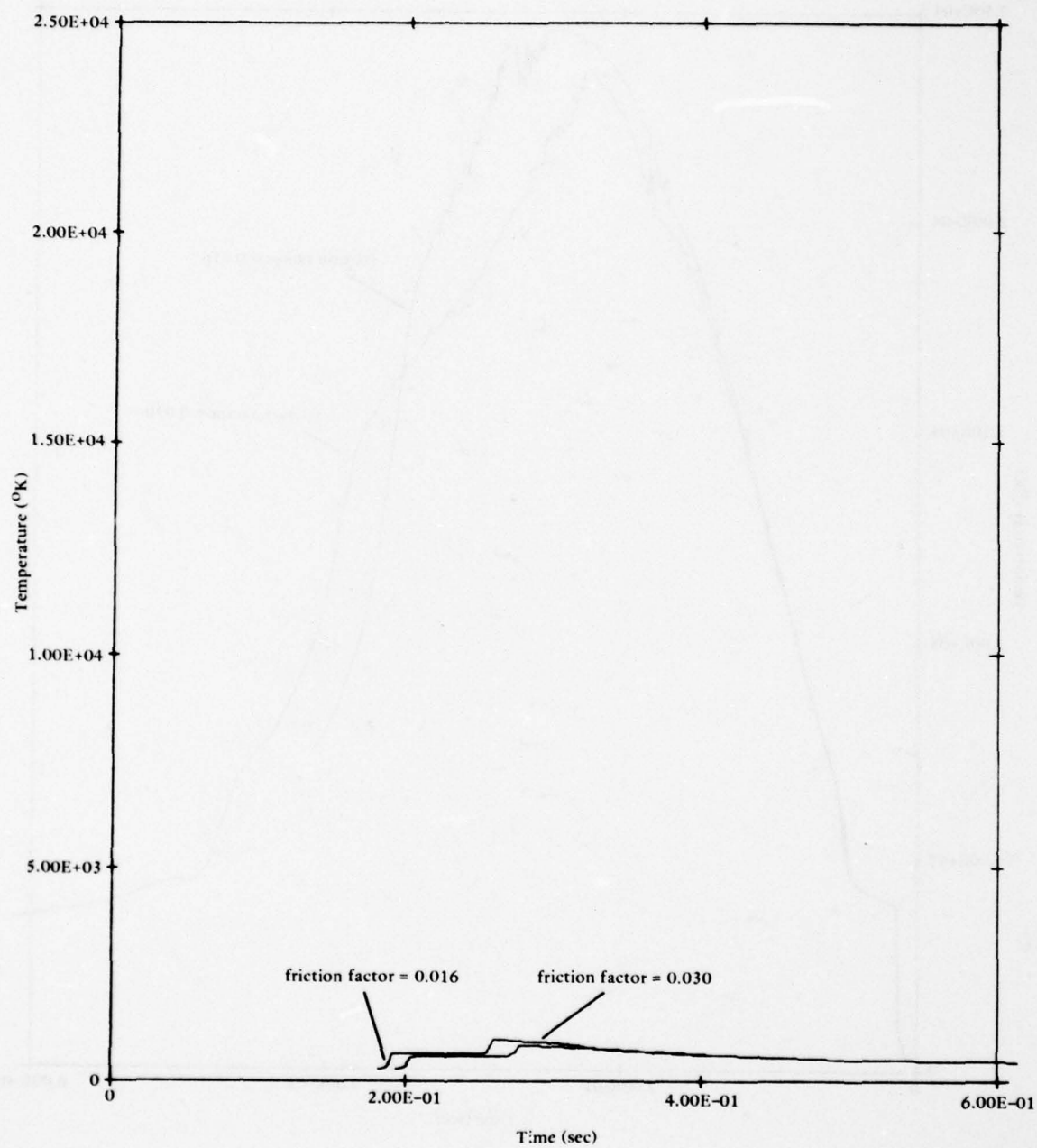


Figure 9b. Temperature-time history for duct station F.

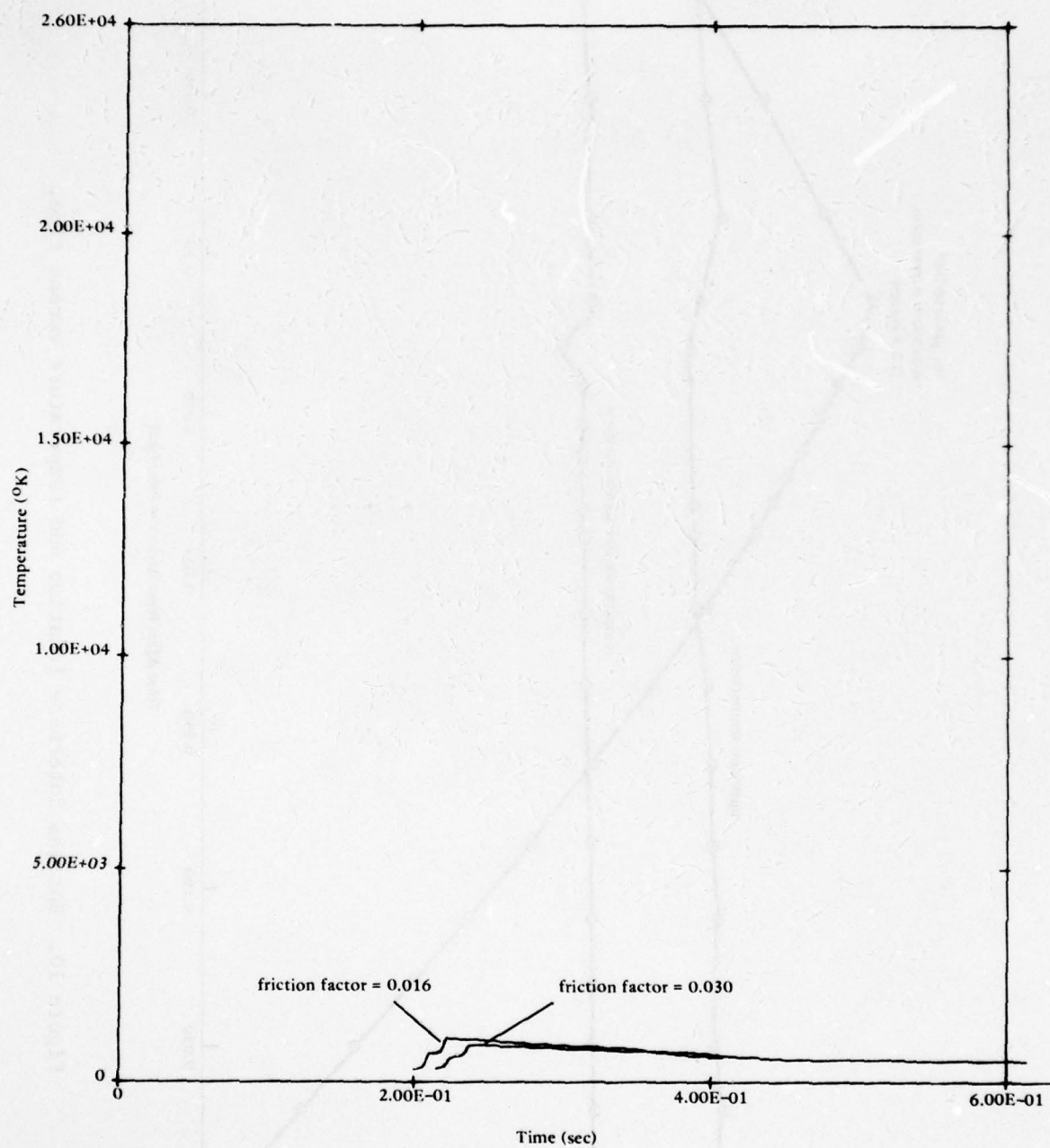


Figure 9c. Temperature-time history for duct station 3.

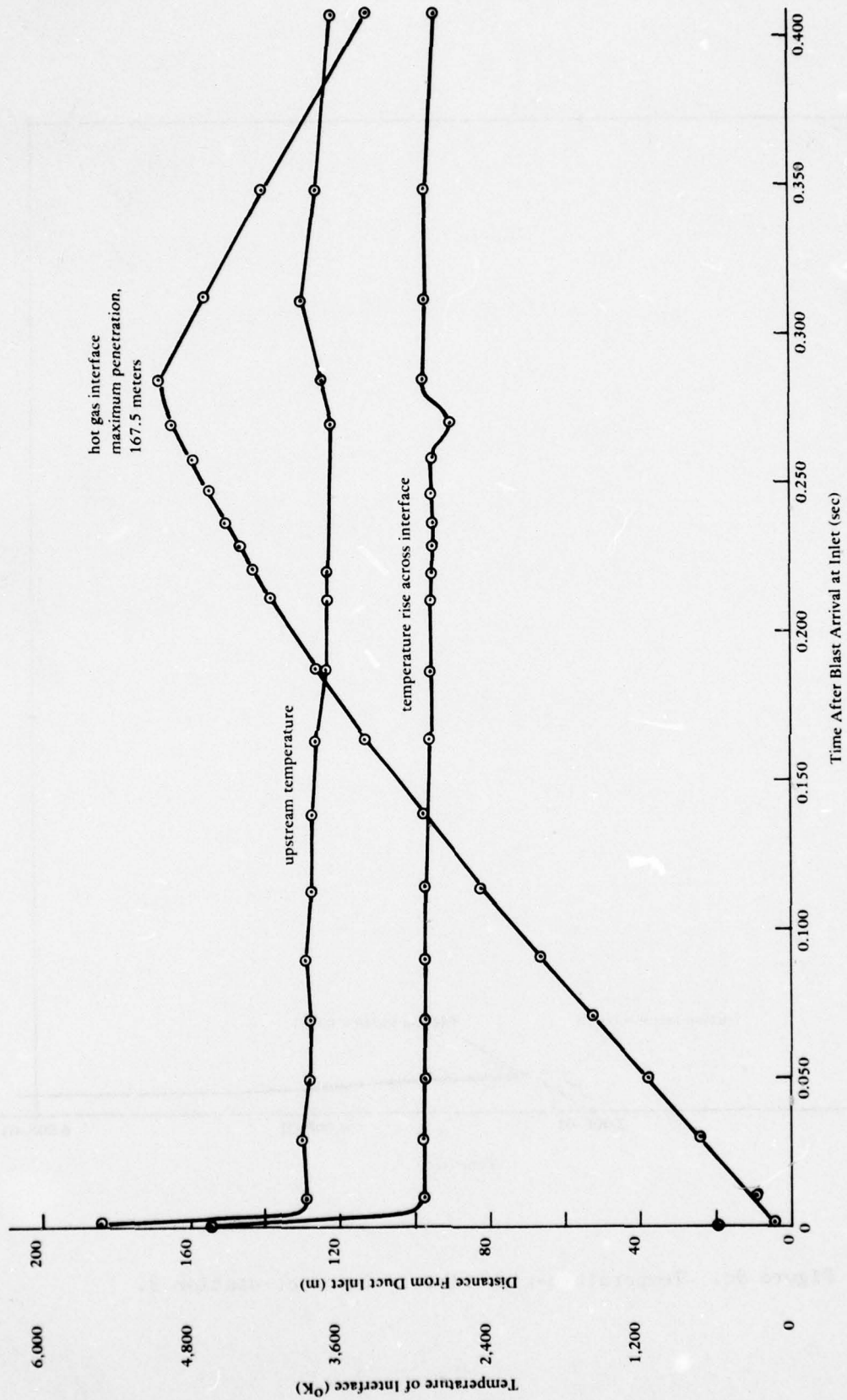


Figure 10. Hot gas interface location and temperature versus time.

Appendix

LAGRANGE COMPUTER CODE DESCRIPTION

INTRODUCTION

The basic structure of the Lagrange computer code and the input and output formats are described below. The computer code listing and card deck can be obtained by requesting a program tape from the Computer Center, Code L06, CEL. All quantities in the code are given in cgs units except for printout of pressure which is given in psia.

CODE BASIC STRUCTURE

The computer code consists of a main control subroutine with several auxiliary subroutines. A list of these subroutines with a description of each function follows.

| <u>Subroutine</u> | <u>Function</u> |
|-------------------|---|
| MAIN | Controls main logical flow and reads input data. |
| BDY 1 | Dummy subroutine, no longer used. |
| BDY123 | Dummy subroutine, no longer used. |
| BDY 2 | Specifies motion of interface at a duct exit (non-nuclear cases). |
| DATEXP | Specifies duct inlet losses using experimental data. |

| <u>Subroutine</u> | <u>Function</u> |
|-------------------|--|
| EQST | Controls equation of state subroutine acquisition. |
| EQS1 | Dummy subroutine, no longer used. |
| EQS3 | Equation of state for real air, $T < 24,000^{\circ}\text{K}$. |
| GENR | Initializes problem. |
| GEOM | Calculates cross-sectional area and zone volume. |
| HTEMP | Calculates Z for EQS3. |
| HYDR | Computes hydrodynamic motions |
| NUBDY | Specifies motion of interface at duct inlet for 1-megaton nuclear wave case. |
| OUT1 | Prints normal output; pressure, etc., in each zone at fixed times |
| OUT2 | Accumulates data on main shock front. |
| OUT3 | Accumulates pressure, etc., versus time at fixed positions. |
| OUT4 | Punches cards from which problem can be continued. |
| REZ1 | Dummy subroutine, no longer used. |
| REZEN1 | Adds a zone at duct entrance for mass inflow. |
| REZENI | Dummy subroutine, no longer used. |
| REZEX1 | Dummy subroutine, no longer used. |
| TIMEST | Calculates time step. |

CODE INPUT QUANTITIES AND FORMATS

The input data symbols, including the data card number on which they appear, and the data format are given in Table 2. The data appears on a particular card in the order in which it is given. A sample data

card listing is given in Table 3 for a 457-meter (1,500-foot) radius location from a 1-megaton nuclear surface burst with a duct system geometry as shown in Figure 6.

CODE OUTPUT VARIABLES AND FORMATS

The output of this computer code consists of printout of the input data, OUT1 subroutine, OUT2 subroutine printout, and OUT3 subroutine printout. The OUT4 subroutine punches cards. To give a full output would be too lengthy; therefore, only a sample output from printout of the input data and OUT1 at cycle 500 are given in Tables 4 and 5, respectively. The data in Tables 3 through 5 are for the example case of Figure 6 in the main body of the report. The program was run on a CDC6600 computer and required a core storage of 130,000. The normal output is provided by the OUT1 subroutine, which prints out the velocity, displacement, and several state variables for each zone at desired times. The printout is controlled by the quantity NPR.

An auxiliary output is provided by the OUT3 subroutine, which prints out variables at the desired locations in the duct versus time. The control variable $S(I,J)$ specifies the location at which the variables are printed out.

Table 2. Input Quantities

| Card Number | Format | Symbol | Definition |
|-------------|--------|----------------------|--|
| 1 | 7A10 | ALIST(I) | Problem definition. |
| 2 | 7A10 | ALIST(I) | Problem definition continued. |
| 3 | 12I5 | NPROB | Problem number. |
| | | IMAXL | =1 |
| | | INTAPE | =0, no data input from tape 18. |
| | | INCODES | =0, no extra input from cards. |
| | | NQUIT | Total number of cycles to run. |
| | | NPR | Print after every NPR cycle(s). |
| | | NTAPE | =0, do not write on tape 18. |
| | | KOPT | =1, side-on entrance (nuclear case) =0, wave originates at entrance |
| 4 | 12I5 | KOUT2 | =0, do not call OUT2 (usually 4 when OUT2 used) |
| | | KOUT2A | Store data every KOUT2 cycles |
| | | KOUT2B | Controls coupling between OUT2 and OUT3; usually zero |
| | | KOUT3A | Store P-T data every KOUT3 cycles |
| | | KOUT4 | Punch continuation cards at KOUT4 cycles |
| | | KREZ1 | =0, REZ1 not used |
| 5 | 12I5 | NC(1) through NC(12) | Control variables, all zero except NC(4), NC(5), NC(6) and NC(7) |
| | | NC(4), NC(5) | =1, always |
| | | NC(6) | =1, print NC(6) times per decade in time |
| | | NC(7) | =1, use special pseudo-viscosity |

(continued)

Table 2. Continued

| Card Number | Format | Symbol | Definition |
|-------------|--------|--|---|
| 6 | 12I5 | NC(13) through NC(24) NC(16), NC(17) | Control variables, all zero except NC(16) and NC(17), always 1 =1, always |
| 7 | 7E10.4 | EBI T DTMIN(2) DTRATE STABIL UCUT | =0, not used =0, start with time zero =0, use built-in time step =0, use built-in time step change rate of 1.4 =0, use built-in stability constant of 0.81 =0, use built-in velocity cut-off of 10^2 cm/sec |
| 8 | 7E10.4 | A-1 through A-5 | Surface wave constants (nuclear case) |
| 9 | 7E10.4 | B-1 through B-7 | Surface wave exponents (nuclear case) |
| 10 | 7E10.4 | DP DU TS TB PSO QSO | Positive phase duration of over-pressure, surface wave Positive phase duration of velocity of surface wave Shock arrival time of surface wave Time of maximum temperature after shock arrival Initial value of pressure wave Initial value of dynamic pressure |

(continued)

Table 2. Continued

| Card Number | Format | Symbol | Definition |
|-------------|------------------|--|--|
| 11 | 7E10.4 | TMPS1 | Surface temperature constant |
| | | TMPS2 | Surface temperature constant. IF zero, use wave input in polynomial form. |
| | | FLAG | =1, use NUBDY subroutine |
| 12 | 7E10.4 | TLIST(1) through TLIST (6) | All zero, printing controlled by NPR |
| 13 | 7E11.4 | A(1) | Experimental data exponent for duct inlet loss |
| 14 | 8F10.0 | T ₁ T ₂ T ₃ | Specifies times for segmenting time waveforms. Used when inputting wave in form of polynomial for branch duct input. |
| 15-23 | 7E11.4/ E11.4 | COEFF | Constants of 7 th degree polynomials that define PS, TEMPS, and QS. Waveform for each variable specified by three polynomials in accord with times T ₁ , T ₂ , and T ₃ . |
| 24 | 5I5 | I = 1 | Duct identification |
| | | NEQST(1) | Number of equation of state in duct |
| | | JCALC(1) | Number of last interface currently being calculated in duct |
| | | NZONES(1) | Total number of zones in duct |
| | | KOUT3(1) | Store P-T data at KOUT3 locations in duct |
| 25 | 8E10.0 | GAMMA1(1) | Gamma used in duct |
| | | OUTBDY(1) | Length of duct |
| | | EINIT(1) | Initial internal energy in duct |
| | | UINIT(1) | Initial velocity in duct |
| | | DINIT(1) | Initial density in duct |

(continued)

Table 2. Continued

| Card Number | Format | Symbol | Definition |
|--------------|--------|--|--|
| | | FRICT(1) CINQ(1) AINQ(1) | Friction factor 2.0, pseudo-viscosity constant 0.2, pseudo-viscosity constant |
| 26 | 6E10.0 | D0(1) D1(1) D2(1) D3(1) X1(1) X2(1) | Diameter for X(I,J) F X1(1) Linear rate of change of diameter =0, not used =0, not used Begin linear diameter change at X1(1) End linear diameter change at X2(1) |
| 27 | 6E10.0 | S(1,1) through S(1,6) | Positions in duct to collect P-T data by OUT3; zero not used |
| Last Card I5 | | NEXT | =1, read new set of data ≠1, stop; end of computation |

46

Table 4. Printout of Initial Constants (Problem

NUCLEAR BURST, SHOCK MS=7.5, DIAM=3.2808 FT
CEL 06/05/78

[illegible]

Amount of Initial Constants (Problem of Figure 6)

THIS PAGE IS BEST QUALITY PRACTICABLE
FROM COPY FURNISHED TO DDC

NTAPE 0 KUPT 1

KEN1 4

NC(7) 1 NC(8) 0 NC(9) 0 NC(10) 0 NC(11) 0 NC(12) 0

NC(19) 0 NC(20) 0 NC(21) 0 NC(22) 0 NC(23) 0 NC(24) 0

DTRATE -0. STABIL -0. UCUT -0.

A4 3.200000E-01 A5 6.800000E-01

B4 1.500000E+02 B5 3.500000E+02 B6 1.990000E+00 B7 -6.314000E-01

T8 1.830000E-01 PS0 6.894000E+07 WS0 2.000000E+08

-0. -0. -0.

-0.

WS-1, PS-2, TEMPS-2, WS-2

| | | | | |
|----|-----|-----|-----|-----|
| 0. | -0. | -0. | -0. | -0. |
| 0. | -0. | -0. | -0. | -0. |
| 0. | -0. | -0. | -0. | -0. |
| 0. | -0. | -0. | -0. | -0. |
| 0. | -0. | -0. | -0. | -0. |
| 0. | -0. | -0. | -0. | -0. |
| 0. | -0. | -0. | -0. | -0. |
| 0. | -0. | -0. | -0. | -0. |
| 0. | -0. | -0. | -0. | -0. |
| 0. | -0. | -0. | -0. | -0. |

THIS PAGE IS BEST QUALITY PRACTICABLE
FROM COPY FURNISHED TO DDQ

Table 4. Continued

| I | NEWT | JCALC | NZONES | KOUT3 | | |
|---|-------------|-------------|-------------|-------|--|-------------|
| 1 | 3 | 5 | 100 | 3 | | |
| | GAMMA1 | OUTBDY | EINIT | UINIT | | DINIT |
| 1 | 1.40000E+00 | 2.00000E+04 | 2.06800E+09 | 0. | | 1.22560E-03 |
| | D0 | D1 | D2 | D3 | | X1 |
| 1 | 2.00000E+02 | -0. | -0. | -0. | | -0. |
| | S | | | | | |
| 1 | 9.50000E+02 | 1.81000E+04 | 1.97000E+04 | -0. | | -0. |

ABLE

Table 4. Continued

THIS PAGE IS BEST QUALITY PRACTICABLE
FROM COPY FURNISHED TO DDC

| UINIT | DINIT | FRICT | CING | AINQ |
|-------|-------------|-------------|-------------|-------------|
| 0. | 1.22560E-03 | 3.00000E-02 | 2.00000E+00 | 2.00000E-01 |
| 03 | X1 | X2 | | |
| -0. | -0. | -0. | | |
| -0. | -0. | -0. | | |

THIS PAGE IS BEST QUALITY PRACTICABLE
FROM COPY FURNISHED TO DDC

Table 5. OUT1 Subroutine Output Listing (Problem

PROBLEM DUCT 2 CEL 06/05/78
CYCLE TIME(SEC) NEXT TIMESTEP IDT JDT
500 9.74161E-02 2.58544E-04 1 60

PS US TEMPS ZS GAMMAS
1.1978154E+07 1.7123796E+05 1.3661717E+04 2.2406686E+00 1.1597483E+00 6.

| I | J | X(I,J+1) CM | U(I,J+1) CM/SEC | X CENTER CM | DENSITY GM/CC | ENERGY ERG/GM | PQ(I,J) DYNE/SQCM | W(I,J) DYNE/SQCM | P |
|---|----|----------------|--------------------|----------------|------------------|------------------|----------------------|---------------------|---|
| 0 | 0 | 5.13975E+02 | 5.173E+04-0. | -0. | -0. | 5.505E+11 | 1.011E+07-0. | | |
| 1 | 1 | 1.27019E+03 | 5.983E+04 | 8.921E+02 | 1.409E-04 | 4.562E+11 | 1.019E+07 | 0. | |
| 1 | 2 | 2.02882E+03 | 5.646E+04 | 1.650E+03 | 1.762E-04 | 3.789E+11 | 1.012E+07 | 3.88E+04 | |
| 1 | 3 | 2.76452E+03 | 6.204E+04 | 2.397E+03 | 2.274E-04 | 2.956E+11 | 1.022E+07 | 0. | |
| 1 | 4 | 3.41528E+03 | 6.207E+04 | 3.090E+03 | 2.953E-04 | 2.186E+11 | 1.039E+07 | 0. | |
| 1 | 5 | 4.00940E+03 | 6.195E+04 | 3.712E+03 | 4.159E-04 | 1.280E+11 | 1.030E+07 | 1.66E+03 | |
| 1 | 6 | 4.49262E+03 | 6.321E+04 | 4.251E+03 | 5.077E-04 | 9.593E+10 | 1.034E+07 | 0. | |
| 1 | 7 | 4.90256E+03 | 6.364E+04 | 4.698E+03 | 6.115E-04 | 7.921E+10 | 1.036E+07 | 0. | |
| 1 | 8 | 5.25033E+03 | 6.372E+04 | 5.076E+03 | 7.110E-04 | 6.580E+10 | 1.029E+07 | 0. | |
| 1 | 9 | 5.57924E+03 | 6.386E+04 | 5.415E+03 | 7.702E-04 | 5.838E+10 | 1.027E+07 | 0. | |
| 1 | 10 | 5.89850E+03 | 6.368E+04 | 5.739E+03 | 8.046E-04 | 5.462E+10 | 1.029E+07 | 3.73E+03 | |
| 1 | 11 | 6.20322E+03 | 6.320E+04 | 6.051E+03 | 8.438E-04 | 5.038E+10 | 1.027E+07 | 1.09E+04 | |
| 1 | 12 | 6.49472E+03 | 6.276E+04 | 6.349E+03 | 8.575E-04 | 4.841E+10 | 1.018E+07 | 9.96E+03 | |
| 1 | 13 | 6.78508E+03 | 6.333E+04 | 6.640E+03 | 8.687E-04 | 4.671E+10 | 1.007E+07 | 0. | |
| 1 | 14 | 6.84981E+03 | 6.350E+04 | 6.817E+03 | 3.787E-03 | 7.004E+09 | 1.005E+07 | 0. | |
| 1 | 15 | 6.90697E+03 | 6.366E+04 | 6.878E+03 | 4.288E-03 | 6.106E+09 | 1.004E+07 | 0. | |
| 1 | 16 | 6.96111E+03 | 6.378E+04 | 6.934E+03 | 4.528E-03 | 5.748E+09 | 1.002E+07 | 0. | |
| 1 | 17 | 7.01375E+03 | 6.385E+04 | 6.987E+03 | 4.656E-03 | 5.562E+09 | 9.999E+06 | 0. | |
| 1 | 18 | 7.06585E+03 | 6.387E+04 | 7.040E+03 | 4.704E-03 | 5.477E+09 | 9.959E+06 | 0. | |
| 1 | 19 | 7.11801E+03 | 6.384E+04 | 7.092E+03 | 4.700E-03 | 5.451E+09 | 9.908E+06 | 1.47E+03 | |
| 1 | 20 | 7.17055E+03 | 6.376E+04 | 7.144E+03 | 4.665E-03 | 5.457E+09 | 9.847E+06 | 4.06E+03 | |
| 1 | 21 | 7.22368E+03 | 6.363E+04 | 7.197E+03 | 4.614E-03 | 5.477E+09 | 9.774E+06 | 6.91E+03 | |
| 1 | 22 | 7.27748E+03 | 6.345E+04 | 7.251E+03 | 4.556E-03 | 5.498E+09 | 9.688E+06 | 9.51E+03 | |
| 1 | 23 | 7.33196E+03 | 6.324E+04 | 7.305E+03 | 4.499E-03 | 5.512E+09 | 9.593E+06 | 1.13E+04 | |
| 1 | 24 | 7.38709E+03 | 6.302E+04 | 7.360E+03 | 4.446E-03 | 5.519E+09 | 9.491E+06 | 1.16E+04 | |
| 1 | 25 | 7.44278E+03 | 6.282E+04 | 7.415E+03 | 4.402E-03 | 5.516E+09 | 9.390E+06 | 1.03E+04 | |
| 1 | 26 | 7.49892E+03 | 6.267E+04 | 7.471E+03 | 4.367E-03 | 5.506E+09 | 9.298E+06 | 7.62E+03 | |
| 1 | 27 | 7.55537E+03 | 6.258E+04 | 7.527E+03 | 4.342E-03 | 5.490E+09 | 9.218E+06 | 4.57E+03 | |
| 1 | 28 | 7.61199E+03 | 6.260E+04 | 7.584E+03 | 4.329E-03 | 5.470E+09 | 9.153E+06 | 0. | |
| 1 | 29 | 7.66860E+03 | 6.271E+04 | 7.640E+03 | 4.330E-03 | 5.448E+09 | 9.121E+06 | 0. | |
| 1 | 30 | 7.72511E+03 | 6.284E+04 | 7.697E+03 | 4.338E-03 | 5.425E+09 | 9.103E+06 | 0. | |
| 1 | 31 | 7.78150E+03 | 6.291E+04 | 7.753E+03 | 4.347E-03 | 5.399E+09 | 9.081E+06 | 0. | |
| 1 | 32 | 7.83783E+03 | 6.292E+04 | 7.810E+03 | 4.351E-03 | 5.369E+09 | 9.044E+06 | 0. | |
| 1 | 33 | 7.89416E+03 | 6.290E+04 | 7.866E+03 | 4.352E-03 | 5.337E+09 | 8.996E+06 | 9.71E+02 | |
| 1 | 34 | 7.95051E+03 | 6.284E+04 | 7.922E+03 | 4.349E-03 | 5.305E+09 | 8.941E+06 | 2.70E+03 | |
| 1 | 35 | 8.00694E+03 | 6.276E+04 | 7.979E+03 | 4.344E-03 | 5.272E+09 | 8.879E+06 | 4.22E+03 | |

1 Subroutine Output Listing (Problem of Figure 6)

THIS PAGE IS BEST QUALITY PRACTICABLE
FROM COPY FURNISHED TO DDC

| ZS | GAMMAS | HTS | DS | ES |
|-------------|---------------|---------------|---------------|---------------|
| 2406686E+00 | 1.1597483E+00 | 6.3916308E+11 | 1.3632133E-04 | 5.5003911E+11 |

| ENERGY ERG/GM | PQ(I,J) DYNE/SQCM | W(I,J) DYNE/SQCM | PRESSURE PSIA | ZONE MASS GRAMS | TEMP KELVIN | DTZJ SEC | GAM | Z |
|------------------|----------------------|---------------------|------------------|--------------------|----------------|-------------|------|-----------|
| 5.505E+11 | 1.011E+07-0. | | 1.466E+02 | | | | | |
| 4.562E+11 | 1.019E+07 0. | | 1.478E+02 | 3.346E+03 | 1.215E+04 | 1.13E-03 | 1.16 | 2.075E+00 |
| 3.789E+11 | 1.012E+07 3.88E+04 | | 1.462E+02 | 4.198E+03 | 1.052E+04 | 1.47E-03 | 1.15 | 1.895E+00 |
| 2.956E+11 | 1.022E+07 0. | | 1.482E+02 | 5.256E+03 | 9.067E+03 | 1.45E-03 | 1.15 | 1.726E+00 |
| 2.186E+11 | 1.039E+07 0. | | 1.506E+02 | 6.038E+03 | 7.870E+03 | 1.84E-03 | 1.16 | 1.557E+00 |
| 1.280E+11 | 1.030E+07 1.66E+03 | | 1.494E+02 | 7.762E+03 | 6.686E+03 | 1.96E-03 | 1.19 | 1.290E+00 |
| 9.593E+10 | 1.034E+07 0. | | 1.500E+02 | 7.708E+03 | 4.564E+03 | 1.61E-03 | 1.21 | 1.555E+00 |
| 7.421E+10 | 1.036E+07 0. | | 1.502E+02 | 7.875E+03 | 4.339E+03 | 1.58E-03 | 1.21 | 1.360E+00 |
| 6.580E+10 | 1.029E+07 0. | | 1.493E+02 | 7.768E+03 | 4.169E+03 | 1.49E-03 | 1.22 | 1.210E+00 |
| 5.838E+10 | 1.027E+07 0. | | 1.490E+02 | 7.959E+03 | 4.084E+03 | 1.45E-03 | 1.23 | 1.138E+00 |
| 5.462E+10 | 1.029E+07 3.73E+03 | | 1.492E+02 | 8.070E+03 | 4.036E+03 | 1.43E-03 | 1.23 | 1.104E+00 |
| 5.038E+10 | 1.027E+07 1.09E+04 | | 1.488E+02 | 8.078E+03 | 3.960E+03 | 1.36E-03 | 1.24 | 1.069E+00 |
| 4.841E+10 | 1.018E+07 9.96E+03 | | 1.475E+02 | 7.853E+03 | 3.901E+03 | 1.32E-03 | 1.24 | 1.059E+00 |
| 4.671E+10 | 1.007E+07 0. | | 1.461E+02 | 7.924E+03 | 3.849E+03 | 1.31E-03 | 1.25 | 1.050E+00 |
| 7.004E+09 | 1.005E+07 0. | | 1.458E+02 | 7.701E+03 | 9.246E+02 | 5.93E-04 | 1.38 | 1.000E+00 |
| 6.106E+09 | 1.004E+07 0. | | 1.456E+02 | 7.701E+03 | 8.155E+02 | 5.57E-04 | 1.38 | 1.000E+00 |
| 5.748E+09 | 1.002E+07 0. | | 1.454E+02 | 7.701E+03 | 7.712E+02 | 5.45E-04 | 1.39 | 1.000E+00 |
| 5.562E+09 | 9.999E+06 0. | | 1.450E+02 | 7.701E+03 | 7.461E+02 | 5.44E-04 | 1.39 | 1.000E+00 |
| 5.477E+09 | 9.959E+06 0. | | 1.445E+02 | 7.701E+03 | 7.375E+02 | 5.49E-04 | 1.39 | 1.000E+00 |
| 5.451E+09 | 9.908E+06 1.47E+03 | | 1.437E+02 | 7.701E+03 | 7.343E+02 | 5.49E-04 | 1.39 | 1.000E+00 |
| 5.457E+09 | 9.847E+06 4.06E+03 | | 1.428E+02 | 7.701E+03 | 7.350E+02 | 5.47E-04 | 1.39 | 1.000E+00 |
| 5.477E+09 | 9.774E+06 6.91E+03 | | 1.417E+02 | 7.701E+03 | 7.375E+02 | 5.46E-04 | 1.39 | 1.000E+00 |
| 5.498E+09 | 9.688E+06 9.51E+03 | | 1.404E+02 | 7.701E+03 | 7.401E+02 | 5.47E-04 | 1.39 | 1.000E+00 |
| 5.512E+09 | 9.593E+06 1.13E+04 | | 1.390E+02 | 7.701E+03 | 7.420E+02 | 5.49E-04 | 1.39 | 1.000E+00 |
| 5.519E+09 | 9.491E+06 1.16E+04 | | 1.375E+02 | 7.701E+03 | 7.427E+02 | 5.54E-04 | 1.39 | 1.000E+00 |
| 5.516E+09 | 9.390E+06 1.03E+04 | | 1.360E+02 | 7.701E+03 | 7.424E+02 | 5.63E-04 | 1.39 | 1.000E+00 |
| 5.506E+09 | 9.298E+06 7.62E+03 | | 1.347E+02 | 7.701E+03 | 7.412E+02 | 5.73E-04 | 1.39 | 1.000E+00 |
| 5.490E+09 | 9.218E+06 4.57E+03 | | 1.336E+02 | 7.701E+03 | 7.392E+02 | 5.84E-04 | 1.39 | 1.000E+00 |
| 5.470E+09 | 9.153E+06 0. | | 1.328E+02 | 7.701E+03 | 7.366E+02 | 5.96E-04 | 1.39 | 1.000E+00 |
| 5.448E+09 | 9.121E+06 0. | | 1.323E+02 | 7.701E+03 | 7.339E+02 | 5.85E-04 | 1.39 | 1.000E+00 |
| 5.425E+09 | 9.103E+06 0. | | 1.320E+02 | 7.701E+03 | 7.311E+02 | 5.84E-04 | 1.39 | 1.000E+00 |
| 5.399E+09 | 9.081E+06 0. | | 1.317E+02 | 7.701E+03 | 7.278E+02 | 5.91E-04 | 1.39 | 1.000E+00 |
| 5.369E+09 | 9.044E+06 0. | | 1.312E+02 | 7.701E+03 | 7.241E+02 | 5.99E-04 | 1.39 | 1.000E+00 |
| 5.337E+09 | 8.996E+06 9.71E+02 | | 1.305E+02 | 7.701E+03 | 7.201E+02 | 5.99E-04 | 1.39 | 1.000E+00 |
| 5.305E+09 | 8.941E+06 2.70E+03 | | 1.296E+02 | 7.701E+03 | 7.160E+02 | 5.97E-04 | 1.39 | 1.000E+00 |
| 5.272E+09 | 8.879E+06 4.22E+03 | | 1.287E+02 | 7.701E+03 | 7.118E+02 | 5.95E-04 | 1.39 | 1.000E+00 |

THIS PAGE IS BEST QUALITY PRACTICABLE
FROM COPY FURNISHED TO DDG

Table 5. Continued

| | | | | | | | | |
|---|----|-------------|-----------|-----------|-----------|-----------|-----------|--------|
| 1 | 36 | 8.06349E+03 | 6.264E+04 | 8.035E+03 | 4.335E-03 | 5.238E+09 | 8.810E+06 | 5.42E+ |
| 1 | 37 | 8.12017E+03 | 6.251E+04 | 8.092E+03 | 4.324E-03 | 5.204E+09 | 8.736E+06 | 6.51E+ |
| 1 | 38 | 8.17701E+03 | 6.238E+04 | 8.149E+03 | 4.312E-03 | 5.170E+09 | 8.660E+06 | 6.37E+ |
| 1 | 39 | 8.23402E+03 | 6.225E+04 | 8.206E+03 | 4.300E-03 | 5.137E+09 | 8.582E+06 | 6.13E+ |
| 1 | 40 | 8.29118E+03 | 6.212E+04 | 8.263E+03 | 4.289E-03 | 5.105E+09 | 8.510E+06 | 6.06E+ |
| 1 | 41 | 8.34848E+03 | 6.203E+04 | 8.320E+03 | 4.278E-03 | 5.073E+09 | 8.438E+06 | 4.44E+ |
| 1 | 42 | 8.40592E+03 | 6.192E+04 | 8.377E+03 | 4.267E-03 | 5.042E+09 | 8.368E+06 | 4.97E+ |
| 1 | 43 | 8.46348E+03 | 6.181E+04 | 8.435E+03 | 4.259E-03 | 5.012E+09 | 8.306E+06 | 5.08E+ |
| 1 | 44 | 8.52120E+03 | 6.173E+04 | 8.492E+03 | 4.247E-03 | 4.981E+09 | 8.253E+06 | 3.56E+ |
| 1 | 45 | 8.57907E+03 | 6.157E+04 | 8.550E+03 | 4.235E-03 | 4.951E+09 | 8.169E+06 | 7.62E+ |
| 1 | 46 | 8.63709E+03 | 6.146E+04 | 8.608E+03 | 4.225E-03 | 4.921E+09 | 8.102E+06 | 5.12E+ |
| 1 | 47 | 8.69536E+03 | 6.135E+04 | 8.666E+03 | 4.206E-03 | 4.889E+09 | 8.014E+06 | 4.98E+ |
| 1 | 48 | 8.75377E+03 | 6.111E+04 | 8.725E+03 | 4.197E-03 | 4.861E+09 | 7.962E+06 | 1.16E+ |
| 1 | 49 | 8.81237E+03 | 6.115E+04 | 8.783E+03 | 4.183E-03 | 4.832E+09 | 7.878E+06 | 0. |
| 1 | 50 | 8.87121E+03 | 6.099E+04 | 8.842E+03 | 4.166E-03 | 4.801E+09 | 7.806E+06 | 7.06E+ |
| 1 | 51 | 8.92987E+03 | 6.05E+04 | 8.901E+03 | 4.179E-03 | 4.784E+09 | 7.799E+06 | 0. |
| 1 | 52 | 8.98873E+03 | 6.134E+04 | 8.959E+03 | 4.164E-03 | 4.755E+09 | 7.726E+06 | 0. |
| 1 | 53 | 9.04722E+03 | 6.128E+04 | 9.018E+03 | 4.190E-03 | 4.743E+09 | 7.760E+06 | 2.88E+ |
| 1 | 54 | 9.10557E+03 | 6.175E+04 | 9.076E+03 | 4.201E-03 | 4.724E+09 | 7.748E+06 | 0. |
| 1 | 55 | 9.16385E+03 | 6.181E+04 | 9.135E+03 | 4.206E-03 | 4.703E+09 | 7.723E+06 | 0. |
| 1 | 56 | 9.22163E+03 | 6.197E+04 | 9.193E+03 | 4.243E-03 | 4.696E+09 | 7.780E+06 | 0. |
| 1 | 57 | 9.27958E+03 | 6.240E+04 | 9.251E+03 | 4.230E-03 | 4.668E+09 | 7.713E+06 | 0. |
| 1 | 58 | 9.33740E+03 | 6.039E+04 | 9.309E+03 | 4.203E-03 | 4.634E+09 | 7.766E+06 | 1.52E+ |
| 1 | 59 | 9.40779E+03 | 5.139E+04 | 9.373E+03 | 3.507E-03 | 4.264E+09 | 7.238E+06 | 1.36E+ |
| 1 | 60 | 9.50500E+03 | 3.644E+04 | 9.456E+03 | 2.522E-03 | 3.526E+09 | 5.928E+06 | 2.40E+ |
| 1 | 61 | 9.63899E+03 | 1.983E+04 | 9.572E+03 | 1.829E-03 | 2.765E+09 | 4.150E+06 | 2.13E+ |
| 1 | 62 | 9.80827E+03 | 6.626E+03 | 9.724E+03 | 1.448E-03 | 2.284E+09 | 2.434E+06 | 1.11E+ |
| 1 | 63 | 1.00006E+04 | 7.606E+02 | 9.904E+03 | 1.274E-03 | 2.104E+09 | 1.298E+06 | 2.26E+ |
| 1 | 64 | 1.02000E+04 | 2.726E+01 | 1.010E+04 | 1.229E-03 | 2.071E+09 | 1.027E+06 | 8.87E+ |
| 1 | 65 | 1.04000E+04 | 7.157E-01 | 1.030E+04 | 1.226E-03 | 2.068E+09 | 1.014E+06 | 2.27E+ |
| 1 | 66 | 1.06000E+04 | 0. | 1.050E+04 | 1.226E-03 | 2.068E+09 | 1.014E+06 | 5.97E+ |
| 1 | 67 | 1.08000E+04 | 0. | 1.070E+04 | 1.226E-03 | 2.068E+09 | 1.014E+06 | 1.31E+ |
| 1 | 68 | 1.10000E+04 | 0. | 1.090E+04 | 1.226E-03 | 2.068E+09 | 1.014E+06 | 0. |
| 1 | 69 | 1.12000E+04 | 0. | 1.110E+04 | 1.226E-03 | 2.068E+09 | 1.014E+06 | 0. |

DUCT NZONES
1 113

MAXIMUM Q OF AREA 1 IS IN ZONE 60 AT X= 9.4849E+03
MAXIMUM PSI OF AREA 1 IS IN ZONE 4 AT X= 3.0899E+03

NORMAL END REACHED IN MAIN ROUTINE

BLE

THIS PAGE IS BEST QUALITY PRACTICABLE
FROM COPY FURNISHED TO DDG

Table 5. Continued

| | | | | | | | | | |
|----|-----------|-----------|----------|-----------|-----------|-----------|----------|------|-----------|
| 03 | 5.238E+09 | 8.810E+06 | 5.42E+03 | 1.277E+02 | 7.701E+03 | 7.075E+02 | 5.95E-04 | 1.39 | 1.000E+00 |
| 03 | 5.204E+09 | 8.736E+06 | 6.51E+03 | 1.266E+02 | 7.701E+03 | 7.033E+02 | 5.95E-04 | 1.39 | 1.000E+00 |
| 03 | 5.170E+09 | 8.660E+06 | 6.37E+03 | 1.255E+02 | 7.701E+03 | 6.991E+02 | 5.99E-04 | 1.39 | 1.000E+00 |
| 03 | 5.137E+09 | 8.582E+06 | 6.13E+03 | 1.244E+02 | 7.701E+03 | 6.944E+02 | 6.03E-04 | 1.39 | 1.000E+00 |
| 03 | 5.105E+09 | 8.510E+06 | 6.06E+03 | 1.233E+02 | 7.701E+03 | 6.908E+02 | 6.06E-04 | 1.39 | 1.000E+00 |
| 03 | 5.073E+09 | 8.438E+06 | 4.44E+03 | 1.223E+02 | 7.701E+03 | 6.868E+02 | 6.14E-04 | 1.39 | 1.000E+00 |
| 03 | 5.042E+09 | 8.368E+06 | 4.97E+03 | 1.213E+02 | 7.701E+03 | 6.828E+02 | 6.16E-04 | 1.39 | 1.000E+00 |
| 03 | 5.012E+09 | 8.306E+06 | 5.08E+03 | 1.204E+02 | 7.701E+03 | 6.790E+02 | 6.18E-04 | 1.39 | 1.000E+00 |
| 03 | 4.981E+09 | 8.253E+06 | 5.56E+03 | 1.194E+02 | 7.701E+03 | 6.751E+02 | 6.26E-04 | 1.39 | 1.000E+00 |
| 03 | 4.951E+09 | 8.169E+06 | 7.62E+03 | 1.184E+02 | 7.701E+03 | 6.713E+ | 6.18E-04 | 1.39 | 1.000E+00 |
| 03 | 4.921E+09 | 8.102E+06 | 5.12E+03 | 1.174E+02 | 7.701E+03 | 6.676E+02 | 6.28E-04 | 1.39 | 1.000E+00 |
| 03 | 4.889E+09 | 8.014E+06 | 4.98E+03 | 1.162E+02 | 7.701E+03 | 6.634E+02 | 6.33E-04 | 1.39 | 1.000E+00 |
| 03 | 4.861E+09 | 7.962E+06 | 1.16E+04 | 1.153E+02 | 7.701E+03 | 6.599E+02 | 6.18E-04 | 1.39 | 1.000E+00 |
| 03 | 4.832E+09 | 7.878E+06 | 0. | 1.143E+02 | 7.701E+03 | 6.561E+02 | 6.49E-04 | 1.39 | 1.000E+00 |
| 03 | 4.801E+09 | 7.806E+06 | 7.06E+03 | 1.131E+02 | 7.701E+03 | 6.523E+02 | 6.38E-04 | 1.39 | 1.000E+00 |
| 03 | 4.784E+09 | 7.799E+06 | 0. | 1.131E+02 | 7.701E+03 | 6.501E+ | 6.51E-04 | 1.39 | 1.000E+00 |
| 03 | 4.755E+09 | 7.726E+06 | 0. | 1.121E+02 | 7.701E+03 | 6.464E+02 | 6.22E-04 | 1.39 | 1.000E+00 |
| 03 | 4.743E+09 | 7.760E+06 | 2.88E+03 | 1.125E+02 | 7.701E+03 | 6.449E+02 | 6.50E-04 | 1.39 | 1.000E+00 |
| 03 | 4.724E+09 | 7.748E+06 | 0. | 1.124E+02 | 7.701E+03 | 6.425E+02 | 5.96E-04 | 1.39 | 1.000E+00 |
| 03 | 4.703E+09 | 7.723E+06 | 0. | 1.120E+02 | 7.701E+03 | 6.398E+02 | 6.51E-04 | 1.39 | 1.000E+00 |
| 03 | 4.696E+09 | 7.780E+06 | 0. | 1.128E+02 | 7.701E+03 | 6.389E+02 | 6.31E-04 | 1.39 | 1.000E+00 |
| 03 | 4.668E+09 | 7.713E+06 | 0. | 1.119E+02 | 7.701E+03 | 6.353E+02 | 6.00E-04 | 1.39 | 1.000E+00 |
| 03 | 4.634E+09 | 7.766E+06 | 1.52E+05 | 1.104E+02 | 7.701E+03 | 6.311E+02 | 4.56E-04 | 1.39 | 1.000E+00 |
| 03 | 4.264E+09 | 7.238E+06 | 1.36E+06 | 8.527E+01 | 7.701E+03 | 5.840E+02 | 2.64E-04 | 1.39 | 1.000E+00 |
| 03 | 3.526E+09 | 5.928E+06 | 2.40E+06 | 5.121E+01 | 7.701E+03 | 4.878E+02 | 2.59E-04 | 1.40 | 1.000E+00 |
| 03 | 2.765E+09 | 4.150E+06 | 2.13E+06 | 2.935E+01 | 7.701E+03 | 3.853E+02 | 3.35E-04 | 1.40 | 1.000E+00 |
| 03 | 2.284E+09 | 2.434E+06 | 1.11E+06 | 1.919E+01 | 7.701E+03 | 3.183E+02 | 5.19E-04 | 1.40 | 1.000E+00 |
| 03 | 2.104E+09 | 1.298E+06 | 2.26E+05 | 1.555E+01 | 7.701E+03 | 2.932E+02 | 1.09E-03 | 1.40 | 1.000E+00 |
| 03 | 2.071E+09 | 1.027E+06 | 8.87E+03 | 1.477E+01 | 7.701E+03 | 2.885E+02 | 2.69E-03 | 1.40 | 1.000E+00 |
| 03 | 2.068E+09 | 1.014E+06 | 2.27E+02 | 1.471E+01 | 7.701E+03 | 2.882E+02 | 3.33E-03 | 1.40 | 1.000E+00 |
| 03 | 2.068E+09 | 1.014E+06 | 5.97E+00 | 1.470E+01 | 7.701E+03 | 2.882E+02 | 3.36E-03 | 1.40 | 1.000E+00 |
| 03 | 2.068E+09 | 1.014E+06 | 1.31E-01 | 1.470E+01 | 7.701E+03 | 2.882E+02 | 3.36E-03 | 1.40 | 1.000E+00 |
| 03 | 2.068E+09 | 1.014E+06 | 0. | 1.470E+01 | 7.701E+03 | 2.882E+02 | 3.36E-03 | 1.40 | 1.000E+00 |
| 03 | 2.068E+09 | 1.014E+06 | 0. | 1.470E+01 | 7.701E+03 | 2.882E+02 | 3.36E-03 | 1.40 | 1.000E+00 |

89E+03
0849E+03

2

LIST OF SYMBOLS

| | |
|-----------------------|--|
| $A_1, A_2, A_3 \dots$ | Constants (see Ref 4) |
| $a_0, a_1, \dots a_7$ | Coefficients of seventh order polynomial for static pressure |
| $b_0, b_1, \dots b_7$ | Coefficients of seventh order polynomial for dynamic |
| $b_1, b_2, b_3 \dots$ | Constants (see Ref 4) |
| $c_0, c_1, \dots c_7$ | Coefficients of seventh order polynomial for temperature |
| D | Duct diameter |
| D_p^+ | Duration of positive pressure phase |
| D_u^+ | Duration of positive velocity phase |
| e | Internal energy per unit mass |
| e_e | Enthalpy at point e |
| e_s | Surface enthalpy |
| f | A wall friction coefficient |
| h_{ts} | Total enthalpy at point s |
| i | Subscript for initial condition |
| M_e | Mach flow number at point e |
| M_s | Flow Mach number at point s |
| P | Pressure |
| P_{te} | Stagnation pressure at point e |
| P_{ts} | Stagnation pressure at point s |
| p | Pressure |
| p_a | Ambient absolute pressure |
| p_e | Entrance pressure |

LIST OF SYMBOLS
(Continued)

| | |
|----------|--|
| p_o | Initial pressure |
| p_s | Surface pressure |
| p_{so} | Shock peak overpressure at $t = t_s$ |
| p_{te} | Stagnation pressure at point e |
| p_{ts} | Stagnation pressure at point s |
| Q_s | Surface dynamic pressure |
| Q_{so} | Peak dynamic pressure at $t = t_s$ |
| R | Particular gas constant |
| s_e | Entropy at point e |
| s_s | Entropy at surface |
| T | Absolute temperature |
| T_e | Temperature (absolute) at point e |
| T_{pk} | Peak shock temperature |
| T_s | Surface temperature |
| T_{so} | Shock temperature at $t = t_s$ |
| T_{te} | Stagnation temperature at point e |
| T_{ts} | Stagnation temperature at point s |
| t | Time from weapon detonation |
| t_{pk} | Time at which peak shock temperature reached |
| t_s | Shock arrival time after detonation |
| u | Particle velocity |
| u_e | Particle velocity at point e |
| u_s | Surface particle velocity |

LIST OF SYMBOLS (Continued)

| | |
|------------|--|
| V | Volume per unit mass |
| x | Distance along duct |
| Z | Compressibility factor |
| Z_s | Surface function of temperature and density |
| γ | Adiabatic exponent for a real gas |
| γ_e | Ratio of specific heats at point e |
| γ_s | Function of temperature and density ratio of specific heats at the surface |
| ρ | Density |
| ρ_s | Surface density |
| τ | $(t - t_s)/Dp^+$ |
| w | $(t - t_s)/Du^+$ |

DISTRIBUTION LIST

AF HQ PREES Washington DC (R P Reid)
 AFB AF Tech Office (Mgt & Ops), Tyndall, FL; AFCEC/XR, Tyndall FL; CESCH, Wright-Patterson; MAC/DET (Col. P. Thompson) Scott, IL; SAMSO/MNNF, Norton AFB CA; Stinfo Library, Offutt NE
 ARMY BMDSC-RE (H. McClellan) Huntsville AL; DAEN-MCE-D (R L Wight) Washington DC; DAEN-MCE-D Washington DC; ERADCOM Tech Supp Dir. (DELS-D-L) Ft. Monmouth, NJ; Tech. Ref. Div., Fort Huachuca, AZ
 ARMY - CERL Library, Champaign IL
 ARMY CORPS OF ENGINEERS MRD-Eng. Div., Omaha NE; Seattle Dist. Library, Seattle WA
 ARMY ENG DIV ED-CS (S. Bolin) Huntsville, AL; HNDED-CS, Huntsville AL; Hnded-Sr, Huntsville, AL
 ARMY ENG WATERWAYS EXP STA Library, Vicksburg MS
 ARMY ENVIRON. HYGIENE AGCY B620, Edgewood Arsenal MD; Water Qual Div (Doner), Aberdeen Prov Ground, MD
 ARMY MATERIALS & MECHANICS RESEARCH CENTER Dr. Lenoe, Watertown MA
 ARMY MISSILE R&D CMD Redstone Arsenal AL Sci. Info. Cen (Documents)
 ARMY-PLASTEC Picatinny Arsenal (A M Anzalone, SMUPA-FR-M-D) Dover NJ
 ASST SECRETARY OF THE NAVY Spec. Assist Energy (P. Waterman), Washington DC
 CINCLANT Civil Engr. Supp. Plans. Ofr Norfolk, VA
 CINCPAC Fac Engrng Div (J44) Makalapa, HI
 CNM NMAT 08T246 (Dieterle) Wash, DC
 CNO Code NOP-964, Washington DC; OP987J (J. Boosman), Pentagon
 COMOCEANSYSPAC SCE, Pearl Harbor HI
 DEFENSE CIVIL PREPAREDNESS AGENCY J.O. Buchanan, Washington DC
 DEFENSE DOCUMENTATION CTR Alexandria, VA
 DEFENSE INTELLIGENCE AGENCY Dir., Washington DC
 DNA STTL, Washington DC
 DOD Explosives Safety Board (Library), Washington DC
 DOE Dr. Cohen
 DTNSRDC Code 1706, Bethesda MD
 DTNSRDC Code 4121 (R. Rivers), Annapolis, MD
 FLTCOMBATTRACENLANT PWO, Virginia Bch VA
 MARINE CORPS BASE Camp Pendleton CA 92055; Code 43-260, Camp Lejeune NC; M & R Division, Camp Lejeune NC; PWO, Camp S. D. Butler, Kawasaki Japan
 MARINE CORPS HQS Code LFF-2, Washington DC
 MCAS Facil. Engr. Div. Cherry Point NC; Code PWE, Kaneohe Bay HI; Code S4, Quantico VA; J. Taylor, Iwakuni Japan; PWO Kaneohe Bay HI
 NAF PWO Sigonella Sicily; PWO, Atsugi Japan
 NAS CO, Guantanamo Bay Cuba; Code 114, Alameda CA; Code 183 (Fac. Plan BR MGR); Code 18700, Brunswick ME; Code 6234 (G. Trask), Point Mugu CA; Dir. Util. Div., Bermuda; ENS Buchholz, Pensacola, FL; PW (J. Maguire), Corpus Christi TX; PWD Maint. Div., New Orleans, Belle Chasse LA; PWO Belle Chasse, LA; PWO Key West FL; PWO, Dallas TX; PWO, Glenview IL; SCE Lant Fleet Norfolk, VA; SCE Norfolk, VA
 NATL RESEARCH COUNCIL Naval Studies Board, Washington DC
 NAVACT PWO, London UK
 NAVAEROSPREGMEDCEN SCE, Pensacola FL
 NAVCOASTSYSLAB Library Panama City, FL
 NAVCOMMAREAMSTRSTA PWO, Norfolk VA; PWO, Wahiawa HI; SCE Unit 1 Naples Italy
 NAVCOMMSTA Code 401 Nea Makri, Greece; PWO, Exmouth, Australia
 NAVEDTRAPRODEVEN Tech. Library
 NAVEDUTRACEN Engr Dept (Code 42) Newport, RI
 NAVEODFAC Code 605, Indian Head MD
 NAVFAC PWO, Barbados
 NAVFACENGCOM Code 043 Alexandria, VA; Code 044 Alexandria, VA; Code 0451 Alexandria, VA; Code 0454B Alexandria, VA; Code 04B5 Alexandria, VA; Code 1023 (T. Stevens) Alexandria, VA; Code 104 Alexandria, VA; Code 2014 (Mr. Taam), Pearl Harbor HI; Morrison Yap, Caroline Is.
 NAVFACENGCOM - CHES DIV. Code 101 Wash, DC
 NAVFACENGCOM - LANT DIV. Eur. BR Deputy Dir, Naples Italy; RDT&ELO 09P2, Norfolk VA
 NAVFACENGCOM - NORTH DIV. Code 1028, RDT&ELO, Philadelphia PA; Design Div. (R. Masino), Philadelphia PA; ROICC, Contracts, Crane IN
 NAVFACENGCOM - PAC DIV. Code 402, RDT&E, Pearl Harbor HI; Commander, Pearl Harbor, HI

NAVFACENGCOM - SOUTH DIV. Code 90, RDT&ELO, Charleston SC
 NAVFACENGCOM - WEST DIV. Code 04B; 09P/20; RDT&ELO Code 2011 San Bruno, CA
 NAVFACENGCOM CONTRACT AROICC, Point Mugu CA; AROICC, Quantico, VA; Eng Div dir, Southwest Pac,
 Manila, PI; OICC, Southwest Pac, Manila, PI; OICC/ROICC, Balboa Canal Zone; ROICC LANT DIV., Norfolk
 VA; ROICC Off Point Mugu, CA; ROICC, Keflavik, Iceland; ROICC, Pacific, San Bruno CA
 NAVMAG SCE, Guam
 NAVOCEANSYSCEN Research Lib., San Diego CA
 NAVPETOFF Code 30, Alexandria VA
 NAVPGSCOL Code 61WL (O. Wilson) Monterey CA
 NAVPHIBASE CO, ACB 2 Norfolk, VA; Code S3T, Norfolk VA
 NAVREGMEDCEN SCE (D. Kaye); SCE, Camp Pendleton CA
 NAVSCOLCECOFF C35 Port Hueneme, CA
 NAVSEC Code 6034 (Library), Washington DC
 NAVSECGRUACT PWO, Adak AK; PWO, Torri Sta, Okinawa
 NAVSHIPYD; Code 202.4, Long Beach CA; Code 202.5 (Library) Puget Sound, Bremerton WA; Code 404 (LT J.
 Riccio), Norfolk, Portsmouth VA; Code 410, Mare Is., Vallejo CA; Code 440 Portsmouth NH; Code 440, Puget
 Sound, Bremerton WA; Code 440.4, Charleston SC; Library, Portsmouth NH; Tech Library, Vallejo, CA
 NAVSTA CO Naval Station, Mayport FL; CO Roosevelt Roads P.R. Puerto Rico; Maint. Div. Dir/Code 531, Rodman
 Canal Zone; PWD (LTJG.P.M. Motolenich), Puerto Rico; PWO, Keflavik Iceland; PWO, Mayport FL; SCE,
 Guam; SCE, Subic Bay, R.P.; Utilities Engr Off. (LTJG A.S. Ritchie), Rota Spain
 NAVSUBASE LTJG D.W. Peck, Groton, CT
 NAVSUPACT CO, Seattle WA; LTJG McGarrah, Vallejo CA
 NAVSURFWPCEN PWO, White Oak, Silver Spring, MD
 NAVTECHTRACEN SCE, Pensacola FL
 NAVWPNCEN Code 2636 (W. Bonner), China Lake CA; PWO (Code 26), China Lake CA; ROICC (Code 702), China
 Lake CA
 NAVWPNSTA EARLE Maint. Control Dir., Yorktown VA; PW Office (Code 09C1) Yorktown, VA; Security Offr.
 Colts Neck NJ
 NAVWPNSUPPCEN Code 09 Crane IN
 NCBU 405 OIC, San Diego, CA
 NCBC CEL AOIC Port Hueneme CA; Code 10 Davisville, RI; Code 155, Port Hueneme CA; Code 156, Port Hueneme,
 CA
 NMCB 133 (ENS T.W. Nielsen); 5, Operations Dept.; 74, CO; Forty, CO; THREE, Operations Off.
 NORDA Code 440 (Ocean Rsch Off) Bay St. Louis MS
 NRL Code 8400 (J. Walsh), Washington DC; Code 8441 (R.A. Skop), Washington DC
 NSC Code 54.1 (Wynne), Norfolk VA
 NSD SCE, Subic Bay, R.P.
 NTC Commander Orlando, FL
 NUSC Code 131 New London, CT; Code EA123 (R.S. Munn), New London CT
 ONR Code 700F Arlington VA
 PHIBCB I P&E, Coronado, CA
 PMTC Pat. Counsel, Point Mugu CA
 PWC CO Norfolk, VA; CO, Great Lakes IL; CO, Oakland CA; Code 120C (Library) San Diego, CA; Code 128, Guam;
 Code 200, Oakland CA; Code 220 Oakland, CA; Code 220.1, Norfolk VA; Code 400, Pearl Harbor, HI; Code 680,
 San Diego CA; OIC CBU-405, San Diego CA; Utilities Officer, Guam; XO Oakland, CA
 U.S. MERCHANT MARINE ACADEMY Kings Point, NY (Reprint Custodian)
 USCG G-EOE-4/61 (T. Dowd), Washington DC
 USCG ACADEMY LT N. Stramandi, New London CT
 USNA Ch. Mech. Engr. Dept Annapolis MD; PWD Engr. Div. (C. Bradford) Annapolis MD
 CALIFORNIA STATE UNIVERSITY LONG BEACH, CA (CHELAPATI)
 CORNELL UNIVERSITY Ithaca NY (Serials Dept, Engr Lib.)
 DAMES & MOORE LIBRARY LOS ANGELES, CA
 FLORIDA ATLANTIC UNIVERSITY Boca Raton FL (Ocean Engr Dept., C. Lin)
 LEHIGH UNIVERSITY Bethlehem PA (Fritz Engr. Lab No. 13, Beedle); Bethlehem PA (Linderman Lib. No.30,
 Flecksteiner)
 LIBRARY OF CONGRESS WASHINGTON, DC (SCIENCES & TECH DIV)
 MICHIGAN TECHNOLOGICAL UNIVERSITY Houghton, MI (Haas)
 MIT Cambridge MA; Cambridge MA (Rm 10-500, Tech. Reports, Engr. Lib.); Cambridge MA (Whitman)
 NY CITY COMMUNITY COLLEGE BROOKLYN, NY (LIBRARY)
 UNIV. NOTRE DAME Katona, Notre Dame, IN

PURDUE UNIVERSITY Lafayette, IN (CE Engr. Lib)
 SEATTLE U Prof Schwaegler Seattle WA
 SOUTHWEST RSCH INST R. DeHart, San Antonio TX
 STANFORD UNIVERSITY Engr Lib, Stanford CA
 STATE UNIV. OF NEW YORK Buffalo, NY
 TEXAS A&M UNIVERSITY W.B. Ledbetter College Station, TX
 UNIVERSITY OF CALIFORNIA BERKELEY, CA (CE DEPT. GERWICK); DAVIS, CA (CE DEPT. TAYLOR);
 LIVERMORE, CA (LAWRENCE LIVERMORE LAB, TOKARZ)
 UNIVERSITY OF HAWAII Honolulu HI (Dr. Szilard)
 UNIVERSITY OF ILLINOIS Metz Ref Rm, Urbana IL; URBANA, IL (LIBRARY); URBANA, IL (NEWARK);
 Urbana IL (CE Dept, W. Gamble)
 UNIVERSITY OF MASSACHUSETTS (Heronemus), Amherst MA CE Dept
 UNIVERSITY OF MICHIGAN Ann Arbor MI (Richart)
 UNIVERSITY OF NEBRASKA-LINCOLN Lincoln, NE (Ross Ice Shelf Proj.)
 UNIVERSITY OF TEXAS Inst. Marine Sci (Library), Port Arkansas TX
 UNIVERSITY OF TEXAS AT AUSTIN AUSTIN, TX (THOMPSON); Austin, TX (Breen)
 UNIVERSITY OF WASHINGTON Dept of Civil Engr (Dr. Mattock), Seattle WA; SEATTLE, WA (MERCHANT)
 URS RESEARCH CO. LIBRARY SAN MATEO, CA
 ARVID GRANT OLYMPIA, WA
 ATLANTIC RICHFIELD CO. DALLAS, TX (SMITH)
 BECHTEL CORP. SAN FRANCISCO, CA (PHELPS)
 BELGIUM HAECON, N.V., Gent
 BROWN & CALDWELL E M Saunders Walnut Creek, CA
 CANADA Mem Univ Newfoundland (Chari), St Johns
 CF BRAUN CO Du Bouchet, Murray Hill, NJ
 NORWAY DET NORSKE VERITAS (Library), Oslo
 FRANCE Dr. Dutertre, Boulogne
 GLIDDEN CO. STRONGSVILLE, OH (RSCH LIB)
 HUGHES AIRCRAFT Culver City CA (Tech. Doc. Ctr)
 ITALY M. Caironi, Milan
 MCDONNELL AIRCRAFT CO. Dept 501 (R.H. Fayman), St Louis MO
 NEWPORT NEWS SHIPBLDG & DRYDOCK CO. Newport News VA (Tech. Lib.)
 NORWAY DET NORSKE VERITAS (Roren) Oslo; I. Foss, Oslo; J. Creed, Ski; Norwegian Tech Univ (Brandtzaeg),
 Trondheim
 PORTLAND CEMENT ASSOC. Skokie IL (Rsch & Dev Lab, Lib.)
 RAND CORP. Santa Monica CA (A. Laupa)
 RAYMOND INTERNATIONAL INC. E Colle Soil Tech Dept, Pennsauken, NJ
 SANDIA LABORATORIES Library Div., Livermore CA
 SCHUPACK ASSOC SO. NORWALK, CT (SCHUPACK)
 SHELL OIL CO. HOUSTON, TX (MARSHALL)
 SWEDEN Cement & Concrete Research Inst., Stockholm; GeoTech Inst
 TRW SYSTEMS REDONDO BEACH, CA (DAI)
 UNITED KINGDOM Cement & Concrete Assoc Wexham Springs, Slough Bucks; Cement & Concrete Assoc. (Lit.
 Ex), Bucks; D. Lee, London; D. New, G. Maunsell & Partners, London; Taylor, Woodrow Constr (014P),
 Southall, Middlesex
 WESTINGHOUSE ELECTRIC CORP. Annapolis MD (Oceanic Div Lib, Bryan); Library, Pittsburgh PA
 WISS, JANNEY, ELSTNER, & ASSOC Northbrook, IL (D.W. Pfeifer)
 WOODWARD-CLYDE CONSULTANTS (A. Harrigan) San Francisco
 BROWN, ROBERT University, AL
 BULLOCK La Canada
 F. HEUZE Boulder CO
 CAPT MURPHY Sunnyvale, CA
 R.F. BESIER Old Saybrook CT